

# Guideline for Surface Loading Assessment

November 2025

#### **NOTICE OF COPYRIGHT**

Copyright © 2025 Energy Connections Canada (ECC). All rights reserved. Energy Connections Canada and the ECC logo are trademarks and/or registered trademarks of Energy Connections Canada. The trademarks or service marks of all other products or services mentioned in this document are identified respectively.

#### **DISCLAIMER OF LIABILITY**

In June 2023, the former Canadian Energy Pipeline Association (CEPA) Foundation rebranded to ECC. Among ECC members are previous CEPA pipeline operators who supported the creation of the Development of a Pipeline Surface Loading Screening Process & Assessment of Surface Loading Dispersing Methods.

The mission of ECC is to mobilize the Canadian energy pipeline industry to influence an evolving energy sector and to achieve excellence in all aspects of industry performance: safety, sustainability, integrity, efficiency, and learning. The publication of this document is ECC's contribution to the safe pipeline delivery of energy products to benefit Canadians and the world.

Use of this Guideline described herein is wholly voluntary. The Guideline described is not to be considered an industry standard and no representation as such is made. It is the responsibility of each operator, or other users of this Guideline, to implement practices that suit their specific pipelines, needs, operating conditions, and location.

Knowledge and understanding of pipe and soil interaction and stress distribution continue to grow and develop and, as such, this Guideline is revised from time to time. For that reason, users are cautioned to confer with ECC to determine that they have the most recent edition of this Guideline.

While reasonable efforts have been made by ECC to assure the accuracy and reliability of the information contained in this Guideline, ECC makes no warranty, representation or guarantee, express or implied, in conjunction with the publication of this Guideline as to the accuracy or reliability of this Guideline. ECC expressly disclaims any liability or responsibility, whether in contract, tort or otherwise and whether based on negligence or otherwise, for loss or damage of any kind, whether direct or consequential, resulting from the use of this Guideline. This Guideline is set out for informational purposes only.

References to trade names or specific commercial products, commodities, services, or equipment constitute neither endorsement nor censure by ECC of any specific product, commodity, service or equipment.

The ECC Guideline is intended to be considered as a whole, and users are cautioned to avoid the use of individual sections without regard for the entire document.

# Acknowledgements

The update of the former CEPA document entitled *Development of a Pipeline Surface Loading Screening Process & Assessment of Surface Loading Dispersing Methods* (2009) into this 2025 edition was supported by the following operating companies within Energy Connections Canada:

- FortisBC Energy Inc.
- Husky Midstream
- Pembina Pipeline Corporation
- Plains Midstream Canada ULC
- TC Energy Corporation
- Trans Mountain Corporation

In addition, ECC appreciated individuals within member companies for their review and feedback for this 2025 edition, which was revised by RSI Pipeline Solutions, LLC and Dynamic Risk Assessment Systems, Inc.

# **Contents**

A	CKNOWI	EDGEMENTS	II
E>	(ECUTIV	E SUMMARY	1
1.	INTR	ODUCTION TO THE UPDATED GUIDELINE	2
	1.1	Background	2
	1.2	SCOPE	
2.	GLOS	SSARY	4
	2 1 LIST (	DF SYMBOLS	Δ
		DF ABBREVIATIONS	
3.	LEGA	CY CEPA MODEL	7
4.	PRCI	VALIDATION PROJECT	8
5.		CY CEPA MODEL AND ITS LIMITATIONS	8
6.	ENH	ANCEMENTS TO THE LEGACY CEPA MODEL	9
7.	TECH	INICAL BASIS FOR PROPOSED ENHANCEMENTS	9
8.		HODOLOGY FOR EVALUATION OF SURFACE LOADS	
9.		CTICAL ASSESSMENT CRITERIA	
10		AMPLES	
		A TECHNICAL REFERENCE	
1		ODUCTION	
2	LEGA	CY CEPA MODEL	11
	2.1	LOADS	12
	2.2	OPERATING STRESSES	14
	2.3	SOIL OVERBURDEN	
	2.4	SURFACE LOADING SOIL PRESSURE	
	2.5	HOOP STRESS – LEGACY CEPA EQUATION	
	2.6	IMPACT FACTOR	
	2.7	LONGITUDINAL STRESSES	22
	2.8	LIVE LOAD STRESSES	
	2.9	ADDITIVE AND EQUIVALENT STRESSES	25
	2.10	TIMBER MAT AND SLAB	26
	2.11	MODEL PERFORMANCE	27
3.	PROI	POSED IMPROVEMENTS	28
	3.1	TECHNICAL BASIS FOR THE PROPOSED IMPROVEMENTS	
	3.1.1	2016 Enhancements Proposed by Kiefner & Associates - Reference [25]	28
	3.1.2	2014 and 2018 ENV-6-1 PRCI Project – References [7, 24]	28
	3.1.3	2018 TC Energy Enhancements – Reference [23]	29

	3.1.4	4 2020 TC Energy Enhancements – Reference [22]	29
	3.1.5	5 2020 RSI Model for Protective Measures – Reference [23]	31
	3.1.6		
	3.1.7	7 2024 ASME Cover Depth Study – Reference [29]	31
	3.1.8	8 2024 TC Energy Enhancements – Reference [21]	32
	3.2	SOIL OVERBURDEN	32
	3.3	E' VALUE	38
	3.4	LONGITUDINAL STRESSES	39
	3.5	BEDDING ANGLE	42
	3.6	IMPACT FACTOR	43
	3.7	GENERAL LOAD FOOTPRINT AND CROSSING ANGLE	43
	3.8	VIBRATORY COMPACTOR	45
	3.9	TIMBER MAT AND SLAB	46
	3.10	EFFECT OF ROAD PAVEMENT	49
	3.11	ASSESSING PIPE ANOMALIES FOR SURFACE LOADING	49
	3.11.	.1 Data Requirements for FFS Assessments	51
	3.11.	.2 Metal Loss in Base Metal	52
	3.11.	.3 Metal Loss with Weld Interaction	53
	3.11.	.4 Crack-Like Features	53
	3.11.	.5 Dent, Mechanical Damage, and Deformation Features	54
4	REFE	ERENCES	55
-			

# **Executive Summary**

The 2025 edition of the *Guideline for Surface Loading Assessment* captures published studies completed by the Pipeline Research Council International to validate the original method developed for the former Canadian Energy Pipeline Association. Except for a few cases, the field results of those studies indicated that the model generally led to conservative assessments for straight pipe without imperfections. Since the validation projects, there have been other published works by the industry to improve on different aspects of surface loading assessment, including improved accuracy of assessment and understanding of induced stress distribution acting on buried piping.

This updated Guideline captures enhancements made to date and proposed enhancements to the original model that can further improve accuracy, but some validation may be warranted. A knowledge gap still exists for the surface loading assessment of pipe containing known imperfections, so additional studies or field validation initiatives may be necessary to enhance understanding and to guide the assessment of such cases.

While a "CEPA surface loading calculator" created by Kiefner and Associates to supplement the original model may be available online and can be used as a screening tool with its inherent assumptions and limitations, it is not associated with this revised Guideline. Each pipeline operator can leverage referenced documents and relevant equations provided to build a company-specific tool to assess crossings that may impact its pipelines.

# 1. Introduction to the Updated Guideline

## 1.1 Background

In Canada, new pipelines are required to be installed with a minimum of cover as specified in Clause 4 of CSA Z662:23 based on service fluid and class location designation. While there have not been confirmed pipeline failures attributed solely to induced stress from vehicular crossings over a right-of-way (ROW), frequent vehicular crossings of buried pipelines by agricultural and non-agricultural equipment, where existing depth of cover may have changed over the years, present pipeline integrity concerns. Stresses from vehicular crossings may contribute to incremental damage that could, over time, lead to issues such as circumferential or off-axis cracking and pipe deformation.

Canadian pipeline operating companies are obligated to ensure the movement of agricultural equipment is not impeded for defined agricultural activities<sup>3</sup>, which necessitates the need to have adequate pipeline depth of cover in place to minimize unacceptable induced stresses.

Consequently, in 2005, the Canadian Energy Pipeline Association (CEPA)<sup>4</sup> engaged Kiefner and Associates (Kiefner) to develop a screening process and method to support operating companies in the assessment of surface loads acting on buried pipelines. The assessment method was further refined in 2009.

<sup>&</sup>lt;sup>1</sup> Table 4.9 of Clause 4 in CSA Z662:23 specifies minimum cover for buried pipelines. Clause 3(2) of the *Pipeline Regulation* in British Columbia (effective October 4, 2010) requires a minimum of 0.8 m of cover under agricultural land. Meanwhile, Clause 29(2) of the *Pipeline Rules* in Alberta (in force November 15, 2023) requires an engineering assessment to demonstrate less cover than required by the *Pipeline Rules* or CSA Z662:23 would be acceptable.

<sup>&</sup>lt;sup>2</sup> Based on available published investigation reports as of the date of this Guideline.

<sup>&</sup>lt;sup>3</sup> Subsection 49(1) of the Alberta Energy Regulator's *Pipeline Rules* states the following: "Except where otherwise provided in this section, no person shall operate a vehicle or equipment across a pipeline at a point that is not within the upgraded and traveled portion of a highway or public road without first obtaining consent from the licensee of the pipeline." Section 49(4) then states that "the consent of the licensee under subsection (1) is not required for a vehicular crossing by ... (b) a vehicle used for agricultural operations."

Section 13(1)(b) of the Canadian Energy Regulator Pipeline Damage Prevention Regulations – Authorizations (effective June 19, 2016) states that "the operation across the pipeline of a vehicle or mobile equipment that is used to perform an agricultural activity is authorized if...the point of crossing (b) has not been the subject of a notification under section 7 of the Canadian Energy Regulator Pipeline Damage Prevention Regulations –

Obligations of Pipeline Companies (also effective June 19, 2016). Section 7 of that legislation states the following: "Even if the condition set out in paragraph 13(1)(a) of the Canadian Energy Regulator Pipeline Damage Prevention Regulations – Authorizations is met, when the operation of vehicles or mobile equipment across a pipeline at specific locations for the purpose of performing an agricultural activity could impair the pipeline's safety or security, the pipeline company must identify those locations and notify [affected] persons in writing of those locations."

<sup>&</sup>lt;sup>4</sup> CEPA ceased operations as of December 31, 2021.

## 1.2 Scope

The aim of this updated Guideline is to capture updated research and industry practices relevant to the assessment of crossings of buried pipelines with the following goals:

- Protecting the safety of the public and pipeline company employees,
- Protecting the environment, private and company property, and
- Maintaining the reliable and economical operation of the Canadian pipeline system.

# 2. Glossary

# 2.1 List of Symbols

The following parameters are used in equations referenced in Appendix A Technical Reference:

Variable	Description
$B_d$	Trench width in Marston trench load calculations
- а С	Backfill compaction degree
$C_d$	Marston load coefficient
D D	Outside pipe diameter, mm or inches
e	Euler's number (2.718281)
$e^{(.)}$	The exponential function
	Soil void ratio, dimensionless
e E	
	Pipe modulus of elasticity (Young's modulus), MPa or psi
$E_{concrete}$	Elastic modulus of concrete, MPa or psi
$E_{s}$	Volumetric elastic modulus of soil elastic in contact with a slab
T/	or plate [Equation 26], MPa/mm or psi/in
E'	Modulus of soil reaction, MPa/mm or pounds per cubic inch
F	Point load at the ground surface, representing part of whole of
	the surface loading, kN or lbf
G	Soil specific gravity
H	Soil cover depth over pipeline, m or ft
I	Second moment of area of pipe section (also known as
	moment of inertia), m <sup>4</sup>
$I_F$	Impact factor, dimensionless
k	Soil spring constant, kN/m³ or lbf/in³
$K_0$	Coefficient of lateral soil pressure
K	Rankine active soil pressure coefficient used in Marston trench
	load calculations
$K_b$	Moment parameter (a function of pipe bedding angle),
	dimensionless
$K_z$	Deflection parameter (a function of pipe bedding angle),
	dimensionless
L	Metal loss anomaly length [Equation 53], mm or inches
L	Radius of stiffness, m or ft
$L_r$	Stress ratio in the longitudinal direction [Equation 56],
	dimensionless
$L_r^{cutoff} = \frac{\sigma_f}{\sigma_y}$	Threshold stress ratio [Equation 57], dimensionless
=	Global bending moment in the pipe created by surface
M(x)	loading, kN-m or lbf-ft [Equation 9]
M	The maximum bending moment along the pipe $(\ M(x)\ _{\infty})$ ,
$M_{max}$	kN-m or lbf-ft
D	Uniform external pressure from soil overburden, MPa or psi
$P_0$	
P	Pipe internal pressure, MPa or psi

 $P_{eq}$  Soil pressure acting on pipe due to an equivalent point load,

MPa or psi

 $P_{live}$  Total vertical soil pressure from a crossing vehicle ( $P_{live} =$ 

 $\sum \sigma_z$ ), MPa or psi

 $P_{prism}$  Vertical soil pressure calculated from Prism Load method, MPa

or psi

 $P_{soil}$  Vertical soil pressure on the pipe from overburden, MPa or psi

Horizontal offset between a point load (F) and measurement

point, mm or inches

 $S_e$  Degree of saturation of soil

Pipe wall thickness, mm or inches

 $T_{installed}$  Pipe installed temperature  $T_{operating}$  Pipe operating temperature

u Beam deflection

γ

 $\gamma_d$ 

 $W_d$  Marston trench load from soil overburden for a rigid pipe  $W_c$  Marston trench load from soil overburden for a flexible pipe w(x) Distributed load over pipe in beam-on-elastic-foundation

analysis

lpha Coefficient of thermal expansion of the pipe material Beam-on-elastic-foundation stiffness parameter, 1/m or 1/ft Ratio of metal loss anomaly width (in the circumferential direction) to pipe circumference [Equation 58], dimensionless

Soil unit weight, kN/m<sup>3</sup> or lbf/ft<sup>3</sup>
Dry soil unit weight, kN/m<sup>3</sup> or lbf/ft<sup>3</sup>

 $\gamma_t$  Soil unit weight as a function of soil moisture content, kN/m³

or lbf/ft3

 $\gamma_w$  Unit weight of water, kN/m³ or lbf/ft³

 $\eta$  Anomaly depth to wall thickness ratio, dimensionless

 $heta_0$  Beam slope of deformation

 $\mu'$  Friction coefficient between the trench and backfill soil in

Marston trench load calculations
Poisson's ratio (0.3 for carbon steel)

 $\sigma_f$  Pipe flow stress (average of SMYS and SMTS), MPa or psi  $\sigma_{cH}$  Plastic collapse stress in the circumferential direction

[Equation 50], MPa or psi

 $\sigma_{cL}$  Plastic collapse stress in the longitudinal direction [Equations

54 and 55], MPa or psi

 $\sigma_{equ}$  Equivalent stress from von Mises formula, MPa or psi

 $\sigma_{\!H0}$  Circumferential stress in the pipe due to the soil pressure from

overburden, MPa or psi

 $\sigma_{H~live}$  Circumferential stress in the pipe due to the soil pressure from

live load, MPa or psi

 $\sigma_{H\_max}$  The maximum additive circumferential stress, MPa or psi  $\sigma_{H\_min}$  The minimum additive circumferential stress, MPa or psi  $\sigma_{H\_pressure}$  Hoop stress due to internal pipe pressure, MPa or psi Longitudinal stress from soil overburden, MPa or psi

 $\sigma_{LG}$  Longitudinal bending stress in the pipe from global surface

loading induced bending moment, MPa or psi

 $\sigma_{Ll}$  Longitudinal bending stress in the pipe from through-wall

surface loading induced bending moment, MPa or psi

 $\sigma_{\!L\ live}$  Total longitudinal surface loading induced bending stress with

impact factor, MPa or psi

 $\sigma_{L\_max}$  The maximum additive longitudinal stress, MPa or psi  $\sigma_{L\_min}$  The minimum additive circumferential stress, MPa or psi  $\sigma_{L\_pressure}$  Longitudinal stress due to internal pipe pressure, MPa or psi  $\sigma_{L\_thermal}$  Longitudinal stress due to thermal expansion, MPa or psi

 $\sigma_{tresca}$  Tresca equivalent stress, MPa or psi

 $\sigma_y$  Specified minimum yield strength of pipe, MPa or psi

 $\sigma_z$  Vertical soil pressure at the top of the pipe from a point load

on the ground surface, MPa or psi

(.) \* (.) Convolution operator

## 2.2 List of Abbreviations

AASHTO American Association of State Highway Transportation Officials

ASCE American Society of Civil Engineers

ASME American Society of Mechanical Engineers

AWWA American Water Work Association

CEPA Canadian Energy Pipeline Association

CF Condition factor

CL Lean clay or low plasticity clay

CL-ML Low plasticity silty clay or clayey silt

CP Cathodic protection

DOC Depth of cover

FAD Failure assessment diagram

EFW Electric flash weld

ERW Electric resistance welded

FEA Finite element analysis

FFS Fitness for service

GP Poorly graded gravel

GW Well graded gravel

HRB Highway Research Board

IPC International Pipeline Conference

LF ERW Low-frequency electric resistance welded

ML Low plasticity silt

MOP Maximum operating pressure

OD Pipe outer diameter

PRCI Pipeline Research Council International, Inc

SAW Submerged arc welded

SC Clayey sand

SCC Stress corrosion cracking

SM Silty sand

SME Subject mater expert

SMTS Specified minimum tensile strength

SMYS Specified minimum yield strength

SP Poorly graded sand

SW Well graded sand

TPD Third-party damage

WT Pipe wall thickness

# 3. Legacy CEPA Model

The legacy CEPA surface loading model was developed to support the assessment of induced stresses of vehicle and construction equipment crossing buried pipelines outside permanent road and railway crossings, which can be addressed by API RP 1102.

The CEPA model calculated circumferential stress of the pipe caused by the pressure from the surface load using a modified Spangler-lowa equation. The pressure from the surface load was determined using the Boussineq equation. The longitudinal stress due to local and global bending was estimated using beam-on-elastic-foundation theory. These equations are addressed in the **Technical Reference (Appendix A)**. The resultant hoop stress, longitudinal stress, and combined biaxial stress are then compared to respective limits from a pertinent standard to determine if the induced stress is acceptable and, if not, temporary protective measures would be required.

One acceptance criterion used in the legacy CEPA model was 90% of the pipe specified minimum yield strength (SMYS) based on the Tresca failure stress criterion for design (Clause 4.7 of CSA Z662:23). However, for integrity assessment, this criterion is considered conservative and ECC operating companies have used a range from 90% SMYS to 100% SMYS for allowable stress limit based either on the Tresca or von Mises criterion.

# 4. PRCI Validation Project

The Pipeline Research Council International, Inc. (PRCI) initiated a project to validate the legacy CEPA model through full-scale field experiments.<sup>5</sup> The test specimens included a 609.6mm (24-inch) outside diameter (OD) pipe in sand, another 24-inch OD pipe in loosely placed (dumped) clay, and a 323.9mm (12-inch) OD pipe in compacted clay. These pipes were subjected to surface loading from a dump truck, a bulldozer, a front-end loader, and a vibratory compactor, with 0.6 m and 0.9 m (2 and 3 feet) depths of cover.

The study found that stress levels in shallow buried pipelines can approach or exceed the fatigue endurance limit of a typical line pipe and that dynamic effects dominated the results from the vibratory compactor tests. While the validation project revealed some discrepancies between the model's assumptions and the experimental data, the legacy CEPA model generally provided a conservative upper bound for hoop stress and for longitudinal stresses. Recommendations from the PRCI project are summarized in Appendix A.

# 5. Legacy CEPA Model and its Limitations

As noted in published works by PRCI ([7] and [20]) and TC Energy ([21], [22], and [23]), the legacy CEPA model had several limitations, as summarized below:

- The pipeline was assumed to be free from anomalies such as metal loss, crack-like features, and dents.
- The pipeline was assumed to be straight without bends.
- The model had not been validated for pipeline cover depths less than 0.9 m (3 ft).
- The soil was assumed to be not very weak.
- The associated CEPA Calculator [4] developed based on the model lacked an explicit option to define a crossing angle (though it could analyze crossing angles other than a 90-degree crossing by using the load matrix option).

<sup>&</sup>lt;sup>5</sup> Details of the study and results are found in the following PRCI reports:

Catalog No. PR-218-104509-03 "Field Validation of Surface Loading Stress Calculations for Buried Pipelines Milestone 1 Report" (July 23, 2014)

Catalog No. PR-218-104509-R01 "Field Validation of Surface Loading Stress Calculations for Buried Pipelines Milestone 2 Report" (April 10, 2018)

<sup>•</sup> Catalog No. PR-218-174512-R01 "Full-Scale Surface Loading Testing of Buried Pipes" (June 21, 2021)

- The equation for spring constant used for the beam-on-elastic-foundation calculations (discussed in Appendix A) appeared to have a unit inconsistency.
- It had limited capabilities for the analysis of crossings with timber-mat, slab, and road plate.
- The prism load model, incorporated into the CEPA model, gave unrealistically high stresses for a deeply buried pipeline.
- The modulus of soil reaction relationship with depth of cover was discontinuous.

# 6. Enhancements to the Legacy CEPA Model

Section 3 of Appendix A summarizes published works that discussed enhancements made since the publication of the legacy CEPA model. Noticeably, TC Energy published several International Pipeline Conference (IPC) papers<sup>6</sup> to explain its approach and methodology in addressing gaps in the legacy CEPA model.

# 7. Technical Basis for Proposed Enhancements

Section 3.1 of Annex A discusses the rationale for some implemented and proposed enhancements.

# 8. Methodology for Evaluation of Surface Loads

Section 2 of Annex A provides the equations necessary to determine if induced stress from a surface load is acceptable or not. If a proposed crossing over an existing pipeline cannot avoid pipe without known imperfections (e.g., corrosion, dents, or cracks), refer to Section 3.10 for some guidance. Protective measures, discussed in Section 3.9 of Appendix A and in other referenced source documents, may be needed to accommodate such cases.

# 9. Practical Assessment Criteria

The improvements proposed in Section 3 of Appendix A address some of the limitations with the legacy CEPA model and can be used when the following conditions are met:

<sup>&</sup>lt;sup>6</sup> Paper No. IPC2018-78633 "Practical Improvements to Surface Loading Assessment – Building Accuracy, Efficiency and Transparency," Paper No. IPC2020-9478 "Improved Surface Loading Stress Analysis Method Considering Protection Measures," and Paper No. IPC2024-133500 "Advanced Surface Loading Stress Analysis Using CEPA Model"

- The pipeline is relatively straight under the crossing. Field bends with angle changes less than about 10 degrees, when they are located outside of crossing footprint, can still be assessed using this method. Operating companies should address situations where fittings and hot bends are present near the crossing, or any bend is present under the crossing. Potential solutions include the use of the model when it can be shown that the model produces acceptable results (for example by conducting numerical analysis on some case studies), or extending the beam-on-elastic-foundation solution used in the model to include pipe bends.
- The pipeline is free from anomalies such as metal loss, crack-like features, dents, mechanical damage, and other types of deformations, unless dedicated FFS assessments are conducted to establish allowable stress limits.
- The pipeline does not experience outside force from other sources unless the effect of those additional forces is included in the analysis.
- The pipeline cover depth is equal to or greater than 0.6 m (2 ft).
- The soil has sufficient bearing capacity to tolerate the weight of the crossing vehicles without allowing the wheels or tracks of the vehicle to penetrate the ground surface.
- The soil classification and conditions are well understood, or very weak soil shear strength with a
  modulus of soil reaction (E') value of 200 psi to 500 psi and a bedding angle of 0 to 30 degrees is
  assumed.

# 10. Examples

The IPC papers mentioned in Section 6 included examples and case studies that illustrated the application of relevant calculations associated with the current state of surface loading assessment. No specific examples have been included to illustrate the application of the proposed enhancements as they have not been fully tested and validated.

# Appendix A Technical Reference

## 1 Introduction

The development of the CEPA surface loading model was driven by a need for a standardized and practical method to assess the effects of vehicle and construction equipment crossings on buried pipelines. Prior to the CEPA model, the primary methodologies consisted of those developed by Spangler et al. at Iowa State University between 1940 and 1970, as well as the work of Ingraffea et al. at Cornell University (sponsored by the Gas Research Institute) in the late 1980s. The latter work was adopted by the American Petroleum Institute as API RP 1102 [1], Steel Pipelines Crossing Railroads and Highways. These methodologies have served the pipeline industry well for routine crossing assessments, particularly when adequate pipeline burial depths are present. However, they fall short in scenarios where the pipeline is buried at depths of less than 0.9 m (3 ft), where very heavy equipment is expected to cross the pipeline at various angles, and where the pipeline contains stress raisers (such as dents, metal losses, or bends), or where soil properties are insufficiently understood.

API RP 1102 standard had other limitations. It was primarily developed for permanent road and railroad crossings, often with specific requirements for minimum cover depth and truck or train loads (e.g., AASHTO H20) for bored pipelines. This made it difficult to apply to temporary crossings, shallow-cover situations, or to a wider range of vehicles with different tire pressures and ground contact areas, such as those with flotation tires or caterpillar tracks.

Recognizing these gaps and the lack of a simplified, industry-wide approach, CEPA and its member companies initiated a joint industry project. The existing guideline for developing road crossing assessment procedures was created in 2009 for CEPA through a joint effort by specialists at Kiefner and Associates, Inc. and SSD Inc.

# 2 Legacy CEPA Model

When a vehicle crosses a buried pipeline or operates in proximity to the pipe, it induces stress in the circumferential and longitudinal directions of the pipe<sup>7</sup>. Calculation of these stresses, also known as the live load stresses, is the subject of a surface loading stress analysis. The live load stresses add to the normal operating stresses, resulting in a momentary increase in total stresses. Furthermore, the live load stresses can cause fatigue damage to the pipe with the presence of a girth weld and/or seam weld if they repeat frequently.

-

<sup>&</sup>lt;sup>7</sup> The legacy CEPA surface loading models can also be used to analyze added static loads such as a stockpile of goods, parking lots, RV storage facilities, or a new embankment. When the nature of the added load is static, the live load stress could become a long-term loading. In this document the live load stress refers to the added stress from the surface loading, whether the load is moving or static.

The legacy CEPA surface loading model and calculator (referred to as the legacy CEPA Calculator hereafter) was developed between 2006 and 2014 by Kiefner and Associates, Inc. [2], [3], [4]. The CEPA model is based on a modified Spangler-lowa equation [5] for circumferential stress calculations and beam-on-elastic-foundation theory [6] for longitudinal stress.

The legacy CEPA model calculates circumferential stress using a modified Spangler-lowa equation and longitudinal stress using beam-on-elastic-foundation theory.

The CEPA model has been developed and verified [7] for steel pipe. Although the legacy CEPA Calculator that was published in 2014 enables analysts to enter elastic properties for materials other than steel, it remains unclear whether the model can be applied to pipes made of materials other than steel. As such, for plastic and concrete pipes, it is recommended to use models specifically designed and calibrated for these types of pipes, such as the PVC Pipe Design and Installation Manual [8], the PE pipeline handbook published by PPI [9], and the Concrete Pressure Pipe [10].

In the CEPA model, the longitudinal and circumferential stresses are calculated by adding the surface loading-induced stresses and the pipeline operating stresses. The pipeline operating stresses comprise the stresses from internal pressure and those due to differential temperature. The surface loading-induced stress in the circumferential direction of the pipe is characterized by local thorough wall bending. The surface loading-induced stress in the longitudinal direction has two components. The global component is related to the beam bending caused by the vehicle's weight. The local component is induced because the circular cross-section of the pipe becomes oval under the weight of the vehicle, resulting in a transition segment between the circular and oval cross-sections, where through-wall bending is generated.

Soil overburden pressure on the pipe causes the circular cross-section of the pipeline to become ovalized, thereby generating a through-wall bending stress in the circumferential direction. Due to the effect of Poisson's ratio, the overburden soil pressure also creates a longitudinal stress component, which is approximately 30% (because Poisson's ratio in carbon steel is 0.3) of the overburden circumferential stress. Overburden stress in a buried pipeline is typically ignored during pipeline design, as permitted by ASME B31 and similar industry standards. However, for surface loading stress analysis, it is recommended to account for the overburdened soil pressure. For example, API RP 1102 [1] includes the overburden stresses.

#### 2.1 Loads

Surface loading forces on a buried pipeline fall under the general category known as outside force. A pipeline under surface loading experiences operating loads consisting of internal pressure and differential temperature, in addition to the surface loading. Therefore, surface loading stress analysis should include all the effects from the following forces:

- Pipe internal pressure,
- Temperature differential,
- Soil overburden pressure, and
- Surface loading.

Surface loading stress analysis should account for all the operating and surface loading induced stresses and their combinations as shown in Figure 1.

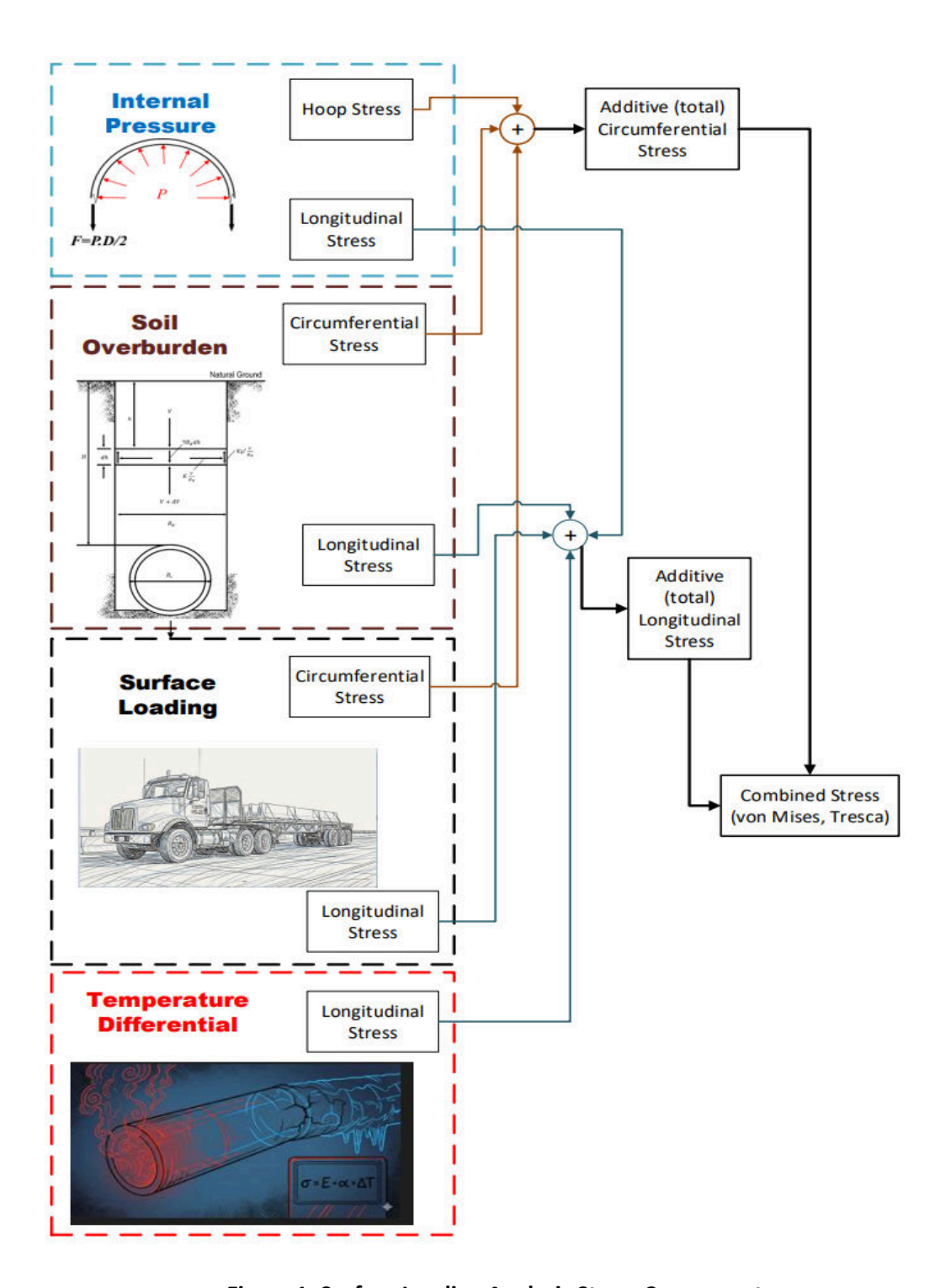


**Figure 1. Surface Loading Analysis Stress Components** 

Analysis of a pipeline requires the following stress components to be calculated:

- 1. Pipe operating stresses
  - a. Hoop stress from pipe internal pressure,  $\sigma_{H\_pressure}$
  - b. Longitudinal stress from pipe internal pressure,  $\sigma_{L\_pressure}$
  - c. Longitudinal stress due to temperature changes,  $\sigma_{L\ thermal}$
- 2. Soil overburden stresses
  - a. Circumferential stress from soil overburden,  $\sigma_{Ho}$
  - b. Longitudinal stress from soil overburden,  $\sigma_{Lo}$
- 3. Live stresses induced by the crossing vehicles
  - a. Live circumferential stress,  $\sigma_{H\ live}$
  - b. Live longitudinal stress,  $\sigma_{L\ live}$
- 4. Additive and equivalent stresses
  - a. Maximum and minimum circumferential stresses which represent the algebraic sums of the above stress components in the circumferential direction
  - b. Maximum and minimum longitudinal stresses which represent the algebraic sums of the above stress components in the circumferential direction
  - c. Equivalent stresses resulting from the combination of the additive circumferential and longitudinal stresses.

Among the above stresses, the operating stresses are calculated directly based on the pipe internal pressure, differential temperature, and mechanical properties of pipe material, including elastic modulus, Poisson's ratio and thermal expansion coefficient.

On the other hand, soil overburden and live stress calculations require vertical soil pressure at the top level of the pipe. Therefore, the calculations of these stresses consist of two analysis stages: first calculate the soil pressure from overburden and crossing vehicles and then calculate the respective stress components. To account for dynamic effects of vehicular forces, an impact factor is applied to the live soil pressure.

The following sub-section describes the analysis processes.

## 2.2 Operating Stresses

The hoop stress due to the pipe internal pressure is calculated using Barlow's equation:

$$\sigma_{H\_pressure} = \frac{P \cdot D}{2t}$$
 Equation 1

Longitudinal stress from internal pressure in a fully restrained pipeline is calculated as follows:

$$\sigma_{L\_pressure} = \frac{P \cdot D}{2t} \nu$$
 Equation 2

In Equation 1 and Equation 2:

P is the pipe internal pressure

D is the pipe outer diameter (OD)

t is the wall thickness of the pipe

 $\nu$  is Poisson's ratio (0.3 in carbon steel)

Longitudinal stress due to thermal expansion in a restrained pipe is calculated as follows:

$$\sigma_{L\_thermal} = -E\alpha (T_{operating} - T_{installed})$$
 Equation 3

where

E is the modulus of elasticity of the pipe

 $\alpha$  is the coefficient of thermal expansion for the pipe

 $T_{installed}$  is the temperature when the pipe was installed

 $T_{operating}$  is the operating temperature of the pipe.

The installation temperature indicates the pipe steel temperature at the time the pipe was fully constrained by the consolidated backfill soil and could be estimated or justified by a subject matter expert (SME). The differential temperature ( $T_{operating} - T_{installed}$ ) is positive when the pipeline operates at a temperature higher than the installation temperature. A positive differential temperature generates compressive stress in the pipe. Conversely, a negative differential temperature generates tensile stress.

#### 2.3 Soil Overburden

A commonly used model to calculate soil overburden pressure is the Prism Load equation:

$$P_{nrism} = \gamma \cdot H$$
 Equation 4

where

 $\gamma$  is the soil unit weight

*H* is the soil cover above the pipe.

Figure 2 shows the concept of soil prism load. The soil pressure in the above equation is the pressure that acts on the outer surface of the pipe upper half. The soil pressure generates circumferential and

longitudinal stress in the pipe. These stresses are calculated using the CEPA equation, which will be discussed in the subsequent sections. The legacy CEPA Calculator has an option for the Trap Door equation [11], [4] in addition to the Prism Load. The Trap Door equation was originally developed by Karl Terzaghi for soil pressure calculation on a tunnel liner therefore it is not deemed appropriate for trench installation (although it can be used for a bored pipe segment) [12]. Other models are available at the time for trench installation (e.g., see [13]), but they were not incorporated into the legacy CEPA Calculator.

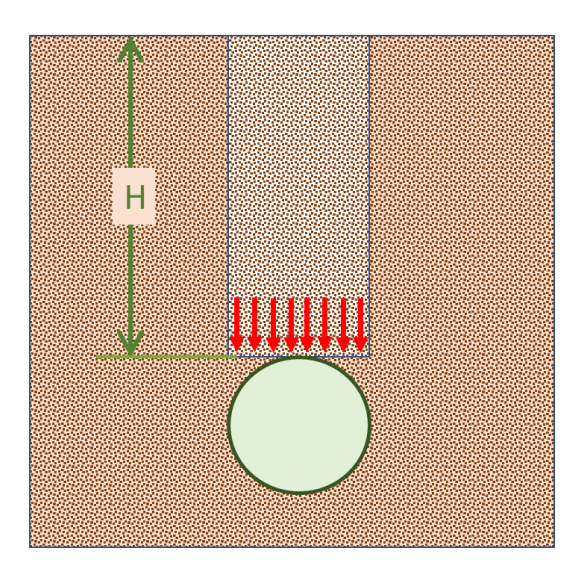


Figure 2. Soil Prism Load

## 2.4 Surface Loading Soil Pressure

Soil pressure on the upper half of the pipe due to the surface loading is calculated using the Boussinesq equation. The Boussinesq equation has an important role in geotechnical stress analysis. The theory was developed by the French mathematician and physicist Joseph Valentin Boussinesq in the late 19th century. His seminal work, Application des Potentiels à l'Étude de l'Équilibre et du Mouvement des Solides Élastiques (1885), provided a solution to a fundamental problem in the theory of elasticity. Boussinesq's solution provided a mathematical formula to calculate the stress field at any point beneath the surface due to a concentrated load. Although the Boussinesq equation is based on simplifying assumptions (e.g., the soil is perfectly elastic and homogeneous), its elegance and practical utility have made it a widely used equation in geotechnical engineering for foundation design and earth pressure analysis. One of the key features of this equation is the principle of superposition which allows the Boussinesq solution to be integrated over a loaded area to determine the stress distribution for more complex loads, such as those from a vehicle's tires or a railway track.

The Boussinesq equation for the vertical soil pressure due to a point load acting on the ground surface is:

<sup>8</sup> https://gallica.bnf.fr/ark:/12148/bpt6k9651115r/f9.item.texteImage

$$\sigma_z = \frac{3F}{2\pi (H)^2 \left(1 + \left(\frac{r}{H}\right)^2\right)^{2.5}}$$
 Equation 5

where

 $\sigma_z$  is soil pressure on the pipe F is point load on ground surface H is depth to the top of pipe r is horizontal offset to where stress is measured

The soil pressure  $(\sigma_z)$  calculated from Equation 5 acts on the upper half of the pipe outer surface. This soil pressure represents the external live load on the pipe. Equation 5 is a linear equation based on the theory of elasticity. Since the equation is linear, the superposition principle can be used to integrate the equation for a general surface loading footprint. In the legacy CEPA Calculator, each vehicle is entered as a matrix of point loads followed by x and y coordinates. The (x,y) coordinate represents the location of each point load on the ground surface. The legacy CEPA Calculator applies the Boussinesq equation to each point load, calculating the soil pressure resulting from the point load. These soil pressures are added up to calculate the total soil pressure acting on the upper half of the pipe. The soil pressure resulting from surface loading is referred to as live load soil pressure. This is referred to as "live" load soil pressure because it is typically associated with the weight of a moving vehicle. The CEPA model can be used for static loads, such as stationary vehicles, the weight of an embankment, or a stockpile. However, when the model is used to analyze a static load, the fatigue check becomes immaterial. It is up to the analyst to decide under what conditions the fatigue check is unnecessary.

The live load soil pressure generates circumferential and longitudinal stresses in the pipe. These stresses are discussed in the subsequent sections. No impact factor, discussed in Sections 2.6 and 3.6, is included in Equation 5.

The applicability of the Boussinesq equation for surface loading analysis of buried pipelines have been experimentally validated by several researches (e.g. [7], [13], [14]).

# 2.5 Hoop Stress – Legacy CEPA Equation

The legacy CEPA model employs the modified Spangler's equation to calculate the circumferential stress in the pipe under vertical soil pressure from soil overburden or surface loading [2], [3]:

$$\sigma_{Ho} = \frac{3K_b \cdot P_{soil} \left(\frac{D}{t}\right)^2}{1 + 3K_z \frac{P}{E} \left(\frac{D}{t}\right)^3 + 0.0915 \frac{E'}{E} \left(\frac{D}{t}\right)^3}$$
 Equation 6

$$\sigma_{H\_live} = \frac{3K_b \cdot I_F \cdot P_{live} \left(\frac{D}{t}\right)^2}{1 + 3K_z \frac{P}{E} \left(\frac{D}{t}\right)^3 + 0.0915 \frac{E'}{E} \left(\frac{D}{t}\right)^3}$$
 Equation 7

where

E is the modulus of elasticity of the pipe

E' is the modulus of soil reaction (Table 1)

 $I_F$  is impact factor

 $K_b$  is a moment parameter which depends on the bedding angle (Figure 3)

 $K_z$  is a deflection parameter which is a function of the bedding angle

P is pipe internal pressure

 $P_{soil}$  Is the vertical soil pressure on the pipe from overburden pressure

 $P_{live}$  is the vertical live soil pressure

t is the pipe wall thickness, and

The remaining parameters are as defined previously.

The stress from Equation 6 is through-wall bending resulting from the ovalization of the pipe cross section, as shown in Figure 4. This stress has opposite signs on the inner and outer surfaces, with a linear gradient through the thickness. The modulus of soil reaction in Equation 6 (E') is an empirical parameter that characterizes the lateral soil stiffness that resists pipe ovalization. Despite its unit, this parameter is generally different from the soil elastic modulus. This parameter has been back-calculated based on measured pipe deflections. Table 1 lists some typical values for the modulus of soil reaction as a function of soil classification, compaction degree, and pipe cover depth. This table is reconstructed from data published by Hartley and Duncan [15]. More information about the modulus of soil reaction can be found in References [5, 15, 16, 17].

When the backfill and native soils differ, the backfill soil characteristics should be used to determine the modulus of soil reaction. The moment and deflection parameters in Equation 6 depend on the pipe bedding angle. Figure 3 shows the concept of the bedding angle schematically. Table 2 contains the moment and deflection parameters for the entire range of bedding angles (0 ° to 180°). Interpolation is used for the in-between values of the bedding angle.

Note that both Equation 6 and Equation 7 are the same equation. The distinction is made because Equation 6 gives the circumferential stress due to the overburden, which is a part of the dead load, while Equation 7 gives the live portion of the stress.

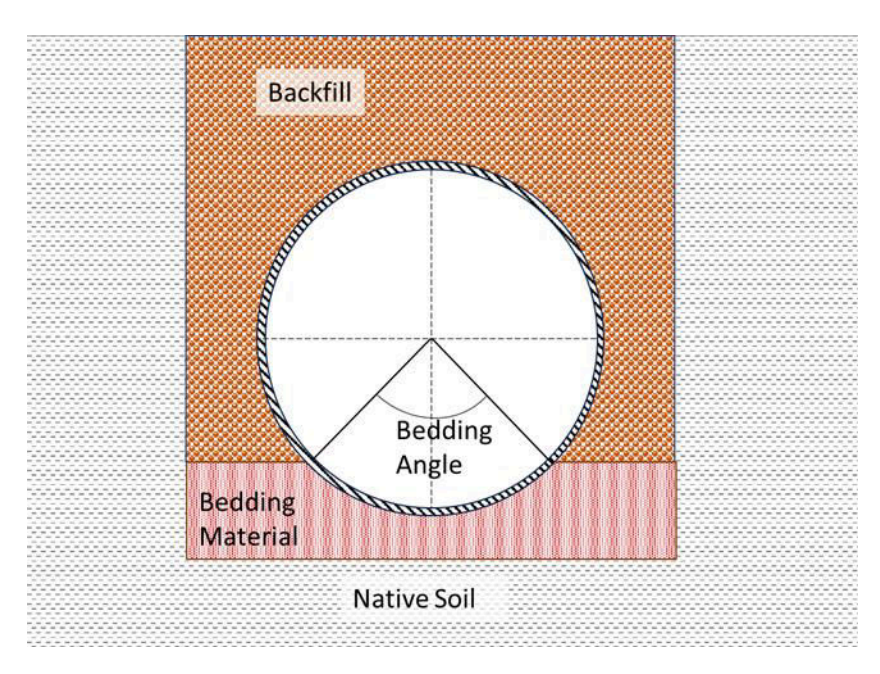


Figure 3. Bedding Angle

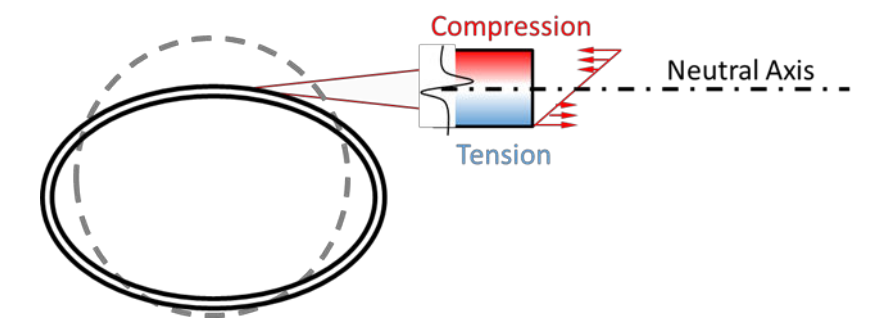


Figure 4. Circumferential Bending due to Pipe Ovalization (Deformation Exaggerated for Demonstration) under Surface Loading

Table 1. Modulus of Soil Reaction (psi)\* [15]

	Depth of	Compaction			
Soil Classification	Cover (ft)	85%	90%	95%	100%
Fine-grained soils with less than 25% sand (CL, ML, CL-ML)	0 - 5	500	700	1000	1,500
	5 - 10	600	1000	1,400	2000
	10 - 15	700	1,200	1,600	2,300
	15 - 20	800	1,300	1,800	2,600
Coarse-grained soils with fines (SM, SC)	0 - 5	600	1,000	1,200	1,900
	5 - 10	900	1,400	1,800	2,700
	10 - 15	1,000	1,500	2,100	3,200
	15 - 20	1100	1,600	2,400	3,700
	0 - 5	700	1,000	1,600	2,500
Coarse-grained soils with little or no fines	5 - 10	1,000	1,500	2,200	3,300
(SP, SW, GP, GW)	10 - 15	1,050	1,600	2,400	3,600
	15 - 20	1,100	1,700	2,500	3,800

<sup>\*</sup> To convert from psi to MPa, divide the values by 145

Table 2. Moment and Deflection Parameters [3]

Bedding Angle, deg	Moment Parameter	Deflection Parameter	
0	0.294	0.110	
30	0.235	0.108	
60	0.189	0.103	
90	0.157	0.096	
120	0.138	0.089	
150	0.128	0.085	
180	0.125	0.083	

The 2005, 2006, and 2009 CEPA reports [2, 3, 18] recommend bedding angles of 0. 30, 60 and  $90^{\circ}$  as follows:

• Consolidated rock: A bedding angle of 0 degrees.

- Open trench conditions: A bedding angle of 30 degrees is typically used and represents an open trench with unconsolidated backfill where the pipe does not have full bearing support. This value is considered a conservative choice for a newly constructed pipeline.
- Bored trench conditions: A bedding angle of 90 degrees.
- Mature pipeline: For a mature pipeline where the soil has re-consolidated around the pipe, a 60-degree bedding angle is used to reflect the additional support. Different soil types require different timeframes to become consolidated. The amount of time required for soil consolidation should be determined by an SME.

The CEPA documents also note that a bedding angle of 30 degrees is the recommended value in many references. For this reason, the user manual of the legacy CEPA calculator, published in 2014 [4] recommends this bedding angle as the default value.

## 2.6 Impact Factor

Live load soil pressure calculated from the Boussinesq equation (Equation 5) is based on the static load of the vehicle. A vehicle crossing over the pipe will result in dynamic loading, therefore the load calculated using the Boussinesq equation is multiplied by an impact factor ( $I_F$ ) to account for the dynamic effects of a moving vehicle, as shown in Equation 7.

Impact factor is usually defined as the ratio of the hoop stresses induced by a dynamic load by that of a static load. Impact factor depends on many factors, some of which are listed below:

- Road surface roughness
- Vehicle's speed
- Whether or not there is a pavement layer
- Pipe cover depth
- Soil and pavement mechanical properties

Field test data conducted by Potter in 1985 under military type vehicles [14] showed:

- Wide scatter in measured impact factors
- An upper limit of 5 for shallow cover depths of less than 0.76m (30 in)
- Highest impact factor observed at vehicular speeds between 8 to 24 kph (5 to 15 mph)
- Higher impact factor from tracked vehicles compared to wheeled vehicles

In the original CEPA model [2, 3, 18, 4], an impact factor of 1.5 was recommended for flexible pavements. This value was based on a recommendation from the ASME committee on Pipeline Crossings of Railways

and Highways. The specification states that an impact factor of 1.5 should be applied to traffic live loads for roads with flexible pavements.

The CEPA report stated that no impact factor was required for roads with rigid pavements at cover depth of 2.1 ft or greater, due to the tendency of rigid pavements to absorb impacts. The reports also state that the American Association of State Highway Transportation Officials (AASHTO) provides specific impact factors for rigid pavements as listed below:

- 1.3 for depths of 0 m.
- 1.2 for depths of 0.03 m to 0.3 m (0.1 to 1.0 feet).
- 1.1 for depths of 0.31 m to 0.61 m (1.1 to 2.0 feet).
- 1.0 for depths of greater than 0.61 m to 0.9 m (2.1 ft to 3.0 feet).

For slow moving equipment with low surface contact pressures (i.e. <30 psi or 206 kPa), a reduced impact factor of 1.25 was recommended. This value meets the AASHTO specification for cover depths greater than 0.3 meters. These types of equipment are designed to have low ground surface pressure to avoid compacting the soil (e.g. agricultural equipment), and typically use low-pressure pneumatic tires, and operate at lower velocities (less than 15 kph or 10 mph).

## 2.7 Longitudinal Stresses

Longitudinal stress from soil overburden is calculated as:

$$\sigma_{Lo} = \nu \cdot \sigma_{Ho}$$
 Equation 8

The global bending stress, which is a part of the live longitudinal stress, is calculated using the beam-onelastic-foundation theory (e.g., see [6]). However, the original CEPA model used a simplified approach in which the vehicle was modeled as an equivalent point load:

$$M(x) = \frac{P_{eq} \cdot D}{4 \cdot \beta^4} \left( 2e^{-\beta \cdot x} \sin(\beta \cdot x) \right)$$
 Equation 9

where

*e* is the Euler's number (2.718281...)

k is soil spring constant per unit length of the pipe

M(x) is the bending surface loading induced moment in the pipe at axial distance x from the selected origin. (The origin for x coordinate is arbitrary but, for ease of calculations, it should be selected near the crossing.)

 $P_{eq}$  is pressure on pipe from an equivalent point load

*I* is the second moment of area for the pipe section

$$\beta$$
 is a beam on elastic foundation parameter defined as  $\beta = \sqrt[4]{\frac{k}{4EI}}$ 

In **Equation 9**, the uniformly distributed pressure on the pipe is caused by an equivalent point load at the surface. This load spreads at a soil distribution angle of 29.9 degrees from the surface point. This simplification was adopted in the original CEPA model from the Highway Line Loads Manual published by the American Concrete Pipe Association [17].

The method for calculating soil spring constant, k, in the original CEPA model was the following:

$$k = E' \cdot D \cdot \theta$$
 Equation 10

Where  $\theta$  is the pipe bedding angle.

Global bending stress in the pipe section is calculated as:

$$\sigma_{LG} = \frac{M_{max}}{I}(0.5D)$$
 Equation 11

**Equation 12** 

In addition to the global bending, the longitudinal stress has a local component which can be calculated from the following equation [19]:

 $\sigma_{Ll} = 0.0981 \sqrt{12(1-v^2)} \cdot \sigma_{H\ live}$ 

Figure 5. Longitudinal Bending from Surface Loading

## 2.8 Live Load Stresses

The live circumferential stress is calculated from Equation 7 as discussed previously. The live longitudinal stress is calculated as the sum of the global and the local bending stresses multiplied by the impact factor,  $I_F$ :

$$\sigma_{L,live} = (\sigma_{LG} + \sigma_{Ll})I_F$$
 Equation 13

The live load stresses can be tensile or compressive, depending on the circumferential location of the stress and whether it is on the inner or outer surface. When a vehicle crosses a buried pipe, the live load stress at a fixed location (e.g., outer surface at 12:00) undergoes a momentary peak. This is shown schematically in Figure 5. Although there are stress reversals before and after each peak, they are of relatively low amplitudes. Thus, live load stresses for fatigue check, as calculated from the above equations, embody the entire stress ranges. On the other hand, depending on the number of axles, the distance between them, and the pipe cover depth, there could be more than one peak associated with each vehicle pass.

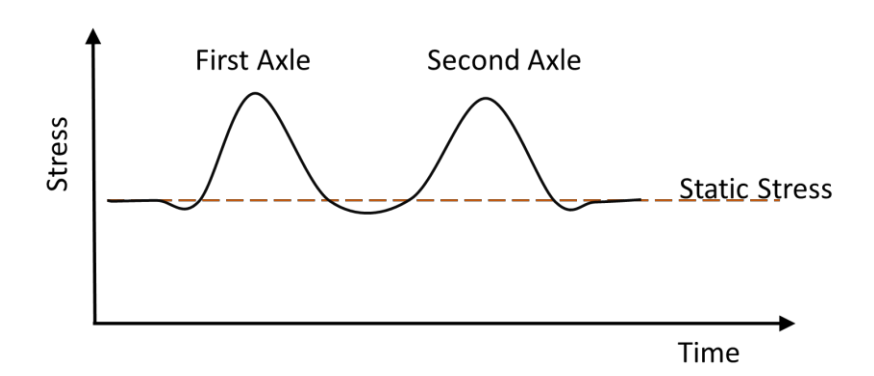


**Figure 6. Surface Loading Induced Live Load Stress** 

Since live load stresses are cyclic in most cases, they should be checked against the material's fatigue limit. For a permanent crossing, the fatigue limits recommended in API RP 1102 [1] can be used and are captured in Table 3. The fatigue endurance limits are pertinent to cyclic loads with a high number of repetitions (e.g., a highway crossing). For a crossing that is temporary in nature (e.g., access to a construction site), the number of repetitions is usually limited; as such, greater stress cycles may become acceptable. In such cases, a full fatigue assessment can be performed to determine the allowable limits.

Table 3. API RP 1102 Fatigue Endurance Limits [1]

Grade	SMYS, psi	Min. Tensile Strength, psi	Girth Weld Fatigue Endurance Limit, S <sub>FG</sub> , psi	Seam Fatigue Endurance Limit, S <sub>FL</sub> , psi		
Grade	31V113, psi			Seamless & ERW	SAW	
A25	25000	45000	12000	21000	12000	
А	30000	48000	12000	21000	12000	
В	35000	60000	12000	21000	12000	
X42	42000	60000	12000	21000	12000	
X46	46000	63000	12000	21000	12000	
X52	52000	66000	12000	21000	12000	
X56	56000	71000	12000	23000	12000	
X60	60000	75000	12000	23000	12000	
X65	65000	77000	12000	23000	12000	
X70	70000	82000	12000	25000	13000	
X80	80000	90000	12000	27000	14000	

## 2.9 Additive and Equivalent Stresses

The circumferential and longitudinal additive stresses are calculated as the sum of the respective stress components:

$$\sigma_{H\_max} = \sigma_{H\_pressure} + \sigma_{Ho} + \sigma_{H\_live} \qquad \qquad \text{Equation 14}$$
 
$$\sigma_{H\_min} = \sigma_{H\_pressure} - \sigma_{Ho} - \sigma_{H\_live} \qquad \qquad \text{Equation 15}$$
 
$$\sigma_{L\_max} = \left(\sigma_{H\_pressure} + \sigma_{Ho}\right) \cdot \nu + \sigma_{L\_max\_thermal} + \sigma_{L\_live} \qquad \qquad \text{Equation 16}$$
 
$$\sigma_{L\_min} = \left(\sigma_{H\_pressure} - \sigma_{Ho}\right) \cdot \nu + \sigma_{L\_min\_thermal} - \sigma_{L\_live} \qquad \qquad \text{Equation 17}$$

In the above equations, the maximum thermal stress is either tensile (positive) or zero, while the minimum thermal stress is either zero or compressive (negative), depending on the differential temperature values entered by the analyst.

The combined equivalent stresses are calculated based on the von Mises and Tresca criteria. The von Mises equivalent stress, which is used in ASME pipeline standards, is calculated in Equation 22 as the greatest of the stresses from Equation 18 through Equation 21:

$$\sigma_{equ1} = \sqrt{\sigma_{H\_max}^2 + \sigma_{L\_max}^2 - \sigma_{H\_max} \cdot \sigma_{L\_max}}$$
 Equation 18
$$\sigma_{equ2} = \sqrt{\sigma_{H\_min}^2 + \sigma_{L\_max}^2 - \sigma_{H\_min} \cdot \sigma_{L\_max}}$$
 Equation 19
$$\sigma_{equ3} = \sqrt{\sigma_{H\_max}^2 + \sigma_{L\_min}^2 - \sigma_{H\_max} \cdot \sigma_{L\_min}}$$
 Equation 20
$$\sigma_{equ4} = \sqrt{\sigma_{H\_min}^2 + \sigma_{L\_min}^2 - \sigma_{H\_min} \cdot \sigma_{L\_min}}$$
 Equation 21
$$\sigma_{equ} = \max(\sigma_{equ1}, \sigma_{equ2}, \sigma_{equ3}, \sigma_{equ4})$$
 Equation 22

The Tresca equivalent stress, which is used by both the ASME and the CSA Z662 pipeline standards, is calculated as:

$$\sigma_{tr1} = \max(\left|\sigma_{H\_max} - \sigma_{L\_min}\right|, \sigma_{H\_max}, \left|\sigma_{L\_min}\right|)$$
 Equation 23
$$\sigma_{tr2} = \max(\left|\sigma_{H\_min} - \sigma_{L\_max}\right|, \left|\sigma_{H\_min}\right|, \sigma_{L\_max})$$
 Equation 24
$$\sigma_{trescq} = \max(\sigma_{tr1}, \sigma_{tr2})$$
 Equation 25

## 2.10 Timber Mat and Slab

The use of timber mat, slab, road plate, and similar tools is among the commonly used means for mitigating surface loading-induced stresses. In the 2009 CEPA report [18] recommended the following equation to calculate the revised surface loading footprint of the dispersed load when such means are utilized:

$$L = \sqrt[4]{\frac{E \cdot h^3}{12(1 - v^2)E_s}}$$
 Equation 26

where

L is radius of stiffness of slab or plate

E is modulus of elasticity of slab or plate

 $E_s$  is described as elastic modulus of soil in contact with slab or plate

h is thickness of slab or plate, and

 $\nu$  is Poisson's ratio of slab or plate

In this model L is the length over which the respective surface load can be distributed. In other words, the equation allows the load to be distributed over a wider area to account for the presence of slab or plate. However, the above equation seems to have inconsistent units, because the right-hand side has the unit of Length to the power of 4/3, while the left-hand side has a unit of length. To resolve this inconsistency,  $E_s$  should be the volumetric modulus with a unit of force per volume (i.e., MPa/mm or psi/in).

#### 2.11 Model Performance

The PRCI project ENV-6-1 [24], [7], launched in 2012, was meant to validate the CEPA model through performing full-scale field experiments. Details of the study can be found in the above PRCI reports. The test specimens included a 24-inch OD, 0.25-inch WT pipe in sand, a 12-inch OD, 0.5-inch WT pipe in compacted clay, and a 24-inch OD, 0.25-inch WT pipe in loosely placed (dumped) clay. These pipes were subjected to surface loading from a dump truck, a bulldozer, a front loader, and a vibratory compactor, with depths of cover of 2 or 3 feet.

The study found that stress levels in shallow-buried pipelines can approach or exceed the fatigue endurance limit of a typical line pipe material. Dynamic effects dominated the results from the vibratory compactor tests.

The validation revealed some discrepancies between the CEPA model's assumptions and the experimental data. For instance, the highest hoop stress location and direction were not always consistent with the assumption of vertical pipe ovalization. Despite these discrepancies, the CEPA model was generally successful in providing a conservative upper bound for hoop stress. Predictions for the 24-inch Sand and 12-inch Packed Clay specimens were conservative in nearly all cases. However, for the 24-inch Dumped Clay specimen, which lacked compaction, the model produced non-conservative predictions in four out of 60 cases, underestimating the hoop stress by as much as 23%.

The study also showed the CEPA model for predicting longitudinal stress. This model was found to be generally conservative, providing an upper bound for longitudinal stresses. Based on the study's findings, the report provides recommendations for selecting model parameters as follows

- 1. Rut depth should be considered when calculating depth of cover (DOC).
- 2. Recommended values for the bedding angle were:
  - a. 90° for clean, non-cohesive soil
  - b. 60° for compacted clay
  - c. 30° for dumped clay

3. An impact factor of 1.5 was found to be appropriate for road vehicles on shallow cover depths (2-3 feet). A higher factor of 2.0 was recommended for construction equipment like bulldozers and front-end loaders. For a vibratory compactor with vibration on, it was recommended to include the centrifugal force with an impact factor of 1 in the analysis.

# 3. Proposed Improvements

The aim of the proposed improvements is to address some of the limitations of the legacy CEPA model.

## 3.1 Technical Basis for the Proposed Improvements

The proposed improvements are primarily based on peer-reviewed research work conducted since the publication of the legacy CEPA Model. These advancements have focused on enhancing the model's accuracy, efficiency, practicality, and versatility.

## 3.1.1 2016 Enhancements Proposed by Kiefner & Associates - Reference [25]

A modified procedure for calculating longitudinal stress and determining soil parameters was introduced in a 2016 paper [25] to address a limitation of the legacy CEPA Model. The new approach uses the modified Spangler stress formula for hoop stress and a more advanced version of the theory of beam-on-elastic-foundation for longitudinal stress, considering both local and global bending. This improved method is suitable for a wider range of scenarios, including open-trench and bored installation methods.

The proposed improvements were validated by comparison with experimental data from 1960-1967 Battelle [26], 1965 Spangler [27] and 1988-1990 Cornell -TTC [28]. The validation showed the model is conservative in predicting the circumferential and longitudinal stresses.

## 3.1.2 2014 and 2018 ENV-6-1 PRCI Project - References [7, 24]

As noted, the PRCI validation project concluded that the legacy CEPA model generally provided a conservative upper bound for surface loading-induced stress in pipelines buried at shallow depths (2 to 3 feet). The following were some key findings from the project:

- The predictions for hoop stress were conservative in almost all cases for the pipe specimen in sand. For the specimen in compacted clay, there was only one non-conservative prediction out of 37 cases. In the non-compacted clay, the model was non-conservative in several cases, with the worst prediction underestimating stress by 23%.
- The model for longitudinal stress was found to be a reliable upper bound, overpredicting stresses by an average factor of 2.8. The study also found that the longitudinal stress model's predictions were conservative for all cases in sand and non-compacted clay. A weak correlation was observed

between longitudinal stress and soil Poisson's ratio, while a strong inverse relationship was found with both soil elastic modulus and cover depth.

- The lack of soil compaction was identified as a major contributing factor to higher-than-expected surface loading-induced stresses. The study showed that live load stresses decreased as soil gained compaction with repeated vehicle passes.
- Pipelines buried in clay experienced greater stress than those in sand in most of the test cases. The horizontal pressure in clay was greater than in sand, demonstrating clay's ability to more effectively transfer pressure horizontally.
- Stress levels decreased with increasing DOC. A 3-inch reduction in DOC was found to increase the predicted hoop stress by about 25%.
- The study confirmed that higher internal pressure reduced live hoop stress. The effect of pipe internal pressure on the live longitudinal stresses was found to be marginal.
- The use of a vibratory compactor with vibration "on" nearly doubled the stresses compared to
  when the vibration was "off". The legacy CEPA model's predictions using the manufacturer's
  specified centrifugal force were generally conservative, suggesting that the force is not fully
  transferred to the ground. Therefore, when the centrifugal force was included in the analysis, an
  impact factor of 1 was recommended.
- The standard published impact factor of 1.5 was found to be appropriate for dump trucks. For shallow DOC, a factor of 2 was recommended for bulldozers and front-end loaders.

## 3.1.3 2018 TC Energy Enhancements – Reference [23]

TC Energy developed an in-house software tool based on the enhanced CEPA model fundamentals published by Kiefner & Associates [25] to improve its practicality. This tool added several advanced functionalities to improve efficiency and accuracy.

The TC Energy tool introduced features such as batch analysis, with the capability to run thousands of cases in a short time, and the ability to model multiple crossing angles from 0 to 90 degrees covering all crossing scenarios from parallel configuration to perpendicular configuration (see Section 3.7 for illustrations). The tool also allowed for generic and site-specific loading analysis, graphical displays of stress distributions, user-defined impact factors, and automated reporting.

TC Energy validated the surface loading analysis tool by comparing its results with both the legacy CEPA calculator and experimental data. The improved longitudinal global bending stress algorithm published in 2016 [25] was shown to be more accurate than the legacy CEPA model predictions.

## 3.1.4 2020 TC Energy Enhancements – Reference [22]

TC Energy introduced a novel methodology to evaluate the effectiveness of temporary protection measures like mats and bridging. This addressed a gap in previous industry tools that did not account for these scenarios.

The paper proposed a modified equation to calculate the "radius of relative stiffness" for mats and an approach to evaluate pipe stress with user-defined bridging free spans. Finite Element Analysis (FEA) validated the new equation for effective length consistent with predicted results.

The paper highlighted that, while industry tools exist for surface loading analysis, they typically do not account for scenarios where pipelines are protected by mats placed on grade or by above-ground bridges. The need for a quantitative method to determine the "effective contact area" of mats was emphasized to ensure safety and cost-effectiveness.

Key methodologies and findings were as follows:

#### 1. Effective Area

- I. <u>Effective Area</u>: FEA revealed that a vehicle load is not distributed across the entire area of a mat. Only a portion of the mat is effective at dispersing the load, and the size of this "effective area" depends on the relative stiffness between the mat and the soil.
- II. <u>Improved Equation</u>: The paper proposes a modified version of the legacy CEPA equation for calculating the radius of relative stiffness (R) that includes the contact width of the tire or track (w). This improved equation was validated against 358 FEA models and was found to be significantly more accurate than the legacy CEPA equation.
- III. <u>Mat Thickness and Soil Stiffness</u>: Parametric analysis showed that increasing the thickness of the mat led to a larger effective area, which in turn reduced ground pressure and live load stresses on the pipe. Similarly, a higher soil modulus of reaction resulted in a larger radius of relative stiffness.

#### 2. Bridging Protection

- I. <u>Simplified Model</u>: The method for analyzing bridging protection (also known as air bridge) simplifies the load to parallel lines, representing the bridge's footings. The pipeline is assumed to be located in the middle of the bridge's free span and perpendicular to the bridge.
- II. <u>Span Length Impact</u>: A key finding from the parametric analysis on bridging was the relationship between the bridge's span length and pipe stress. As the free span increases, the live load stress on the pipe is reduced. However, if the free span is too small, the bridge can concentrate the load and cause higher stresses than if there were no bridge at all. The analysis suggested that the free span should be greater than or equal to the DOC to avoid an adverse impact.

#### 3. Software Tool

A software tool was developed by TC Energy that incorporates these improved methodologies. It allows users to visualize the effective area of the mat and the resulting pressure distribution on the pipe at different crossing angles. This tool also helps in calculating stresses for user-defined bridge free spans, providing flexibility for optimizing protection measures in the field.

## 3.1.5 2020 RSI Model for Protective Measures – Reference [23]

This paper introduced an analytical model to calculate the load distribution on the ground surface from temporary crossings like timber mats and flexible slabs. The model is based on the beam-on-elastic-foundation theory and uses the Laplace transform to find solutions with free-end boundary conditions.

## 3.1.6 2021 ENV-6-2 PRCI Project – Reference [20]

Included in the study was the evaluation of the effectiveness of different temporary crossing methods, such as ground mats, mat bridges, and steel plates, in reducing stress on the pipelines. The following observations were made:

- A single 4-foot-wide mat was generally ineffective at reducing pipe stress and, in many cases, increased them, especially with tracked vehicles. This was attributed to load concentration and impact from the equipment.
- On the other hand, using multiple mats (five side-by-side) or a mat bridge consistently reduced both hoop and longitudinal stresses. For mat bridges, increasing the spacing between supports and increasing the support contact area led to greater stress reduction.
- The orientation of the mats was found to be important for tracked vehicles, and using mats with timber parallel to the pipe was shown to be ineffective at consistently reducing stress.

## 3.1.7 2024 ASME Cover Depth Study - Reference [29]

The study's scope included a review of historical trends in ASME B31 and U.S. regulations, international standards, industry data, risk models, and cost-benefit analysis. It also considered the effects of rock excavation and service conversions.

Data from the U.S., UK, and Europe showed a general decrease in excavation damage incidents over time. This reduction was difficult to link directly to changes in standards or regulations and appeared to be driven more by increased industry awareness. When damage rates were normalized by mileage, incidents were highest at depths less than 24 inches and greater than 48 inches. The lowest damage rates were found in the 24-inch to 36-inch range. The high rate at deeper cover might be due to difficulty in locating and exposing the deeper pipe in construction zones. The study suggested that a combination of engineering, administrative, and behavioral barriers is necessary for effective damage prevention.

FEA of rock excavation trenches showed that surface loading-induced stress on the pipe decreased with greater cover, but the benefit diminished beyond 20 inches of cover. Stress also decreased with a narrower trench (less than twice the pipe diameter) and with increasing wall thickness, particularly for pipes with a diameter-to-wall thickness ratio (D/t) less than 50. These findings were consistent with the Marston Model [13] predictions.

The FEA study showed reasonable agreement with the predictions of the legacy CEPA equation for circumferential stress. It also showed that, in most cases, two inches of a padding layer would be sufficient to prevent damage due to rock fragments.

### 3.1.8 2024 TC Energy Enhancements – Reference [21]

This most recent work focused on addressing frequently asked questions and provided a systematic approach for advanced analysis using the advanced CEPA model. New methodologies were developed for creating generic surface loading conditions not limited to single vehicles and for numerically constructing a 3D live load pressure field using Boussinesq equations. The model now includes a methodology to automatically identify the critical location of a vehicle relative to the pipeline centerline at any given crossing angle, which helps to determine the most critical stresses.

The methodologies for conducting fatigue analysis for girth and seam welds under crossings using the advanced CEPA model in conjunction with API RP 1102 were also addressed, highlighting the importance of the stress analysis model in determining fatigue life.

#### 3.2 Soil Overburden

As noted, the legacy CEPA model used the Prism Load equation (**Equation 4**) for overburden soil pressure calculation:

$$P_{prism} = \gamma \cdot H$$

The Prism Load equation yields conservative results in most cases. This is because the Prism Load only accounts for the vertical soil pressure whereas, in reality, the soil pressure also has a lateral (horizontal) component. In other words, a portion of the soil overburden pressure acts similarly to external hydrostatic pressure (Figure 7). To account for the lateral soil pressure, one can use "the coefficient of earth pressure at rest" or  $K_0$ , (see [11]). For a pipe installed in a backfilled trench this coefficient can be calculated using soil Poisson's ratio:

$$K_0 = \frac{v_{soil}}{1 - v_{soil}} \le 0.55$$
 Equation 27

The effective soil pressure after the application of the lateral soil pressure becomes:

$$P_{soil} = (1 - K_0)P_{prism}$$
 Equation 28

$$P_0 = P_{lateral} = K_0 P_{prism}$$
 Equation 29

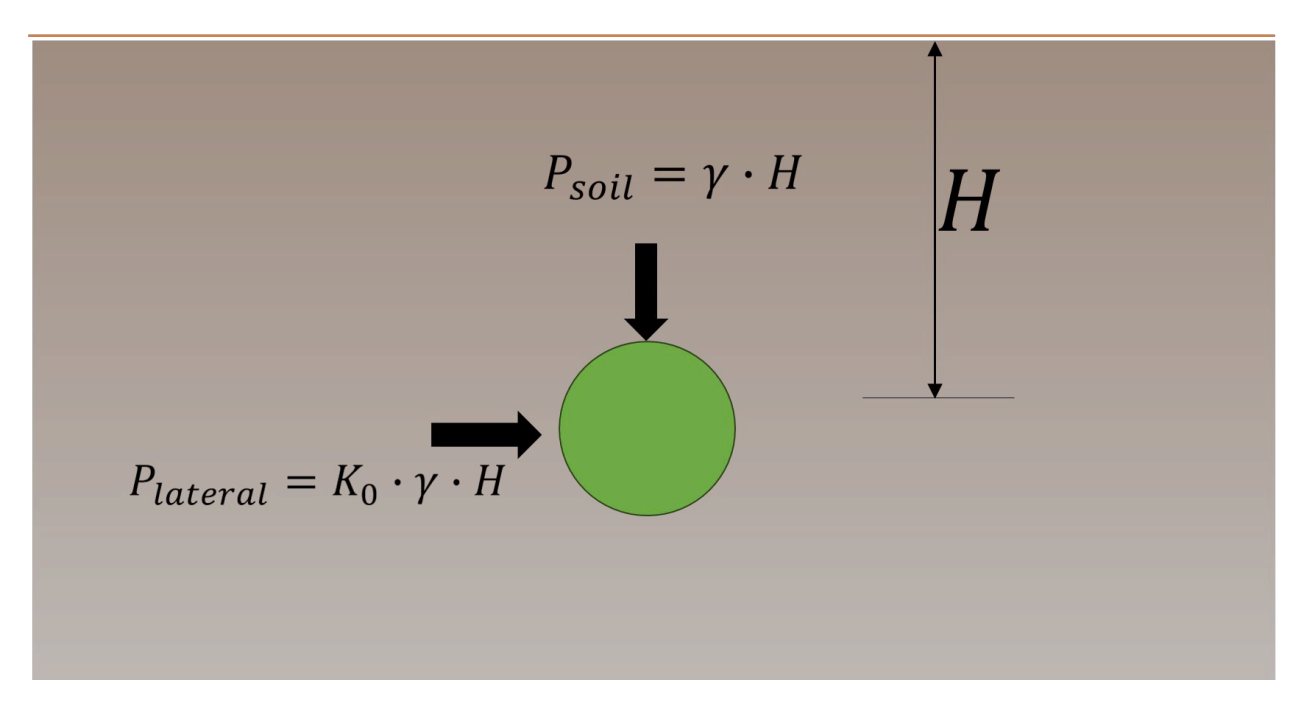


Figure 7. Soil Load Prism with Ko

The soil pressure resulting from **Equation 28** represents the net vertical soil pressure that causes the pipe section to ovalize. The soil pressure in **Equation 29** is the remaining portion of the soil pressure that affects the pipe like external hydrostatic pressure (because it is equal in the vertical and horizontal directions). This soil pressure does not contribute to pipe ovalization but creates a relatively small uniform compression, which can be ignored or calculated using Barlow's equation (Equation 1 with a negative sign). Using  $K_0$  values greater than 0.55 is not recommended unless a dedicated field investigation confirms that the value is representative of the local conditions. The 0.55 limit is based on finite element simulations that were conducted as a part of a cover-depth study sponsored by ASME [29].

Typical values of soil Poisson's ratios are listed in Table 4 for different soil classifications.

Table 4. Typical Values for Soil Poisson's Ratio [30]

Soil Classification	Value
Saturated clay	0.45 to 0.5
Unsaturated clay – stiff	0.20
Unsaturated clay – medium	0.25
Unsaturated clay – soft	0.30
Silt	0.3 to 0.35
Sandy clay	0.2 to 0.3
Dense sand and gravel	0.30
Medium sand and gravel	0.25
Loose sand and gravel	0.15

If a pipe is buried under the water table, the Prism load can be corrected for water pressure as follows:

$$P_{nrism} = \gamma_{sat} \cdot H - u$$
 Equation 30

Where u is the hydrostatic water pressure at the top of the pipe. In Equation 29, the subscript "sat" is introduced to emphasize that the soil unit weight is the saturated unit weight. It is well known in soil engineering that soil unit weight increases with increasing moisture content. The following equation can be used to calculate soil unit weight at different moisture content values [28]:

$$\gamma_t = \frac{(G + S_e)\gamma_w}{1 + e}$$
 Equation 31

Where

e is soil void ratio

G is specific gravity of soil grains, usually about 2.65

 $S_e$  is degree of saturation ( $0 \le S_e \le 1$ )

 $\gamma_t$  is total soil unit weight

 $\gamma_w$  water unit weight

For example, if the unit weight of dry soil ( $\gamma_d$ ) and specific gravity of soil grains are known from soil sampling, **Equation 31** can be used to estimate soil void ratio:

$$\gamma_d = \frac{G \cdot \gamma_w}{1 + \rho}$$
 Equation 32

The soil unit weight at any given degree of saturation can be calculated from this equation. The highest weight is obtained when the soil is completely saturated ( $S_e = 1$ ), in which case:

$$\gamma_t = \frac{(G+1)\gamma_w}{1+e} = \gamma_d + \frac{\gamma_w}{1+e} = \gamma_d + \frac{\gamma_d}{G}$$

Field tests performed by Potter in 1985 [14] on a 10-inch gas pipeline revealed a linear relationship between soil overburden pipe deflections and cover depths ranging from near zero to 30 inches (zero to 0.76 m). This study suggested that the use of prism load for shallow cover depths is appropriate.

Although the Prism load is generally conservative, there are situations where the soil Prism underestimates vertical soil pressure. In general, when the backfill soil is compacted, soil arching tends to reduce the soil overburden, especially for a deep pipeline [28]. However, if the backfill soil above a buried pipe is not compacted, it tends to settle over time, increasing soil overburden pressure due to the rigidity of the pipe relative to the loose soil.

The Marston model is another alternative for calculating soil overburden. This method accounts for the soil friction between the backfill and the sides of the excavated trench. Figure 7 shows the basis for the Marston theory. For a rigid pipe, the load per unit length of the pipeline ( $W_d$ ) is assumed to be equal to the weight of the backfill minus the soil friction along the sides of the ditch. In a flexible pipeline, the load per unit length ( $W_c$ ) is spread over the trench's width. This distribution enables the trench bottom to absorb some of the load, effectively reducing the load per unit length of the pipe. The Marston equations are as follows:

$$W_d = C_d \gamma B_d^2$$
 Equation 33

$$W_c = C_d \gamma D B_d$$
 Equation 34

$$C_d = \frac{1 - e^{-2K\mu'(\frac{H}{B_d})}}{2K\mu'}$$
 Equation 35

Where

 $B_d$  is the trench width

 $C_d$  is load Coefficient

D is the pipe OD

e is the Euler's number (2.718281...)

*H* is pipe Depth of Cover (Soil Cover)

K Rankine active soil pressure coefficient (see Figure 8)

γ is soil unit weight

 $\mu'$  is friction coefficient between the trench and backfill soil

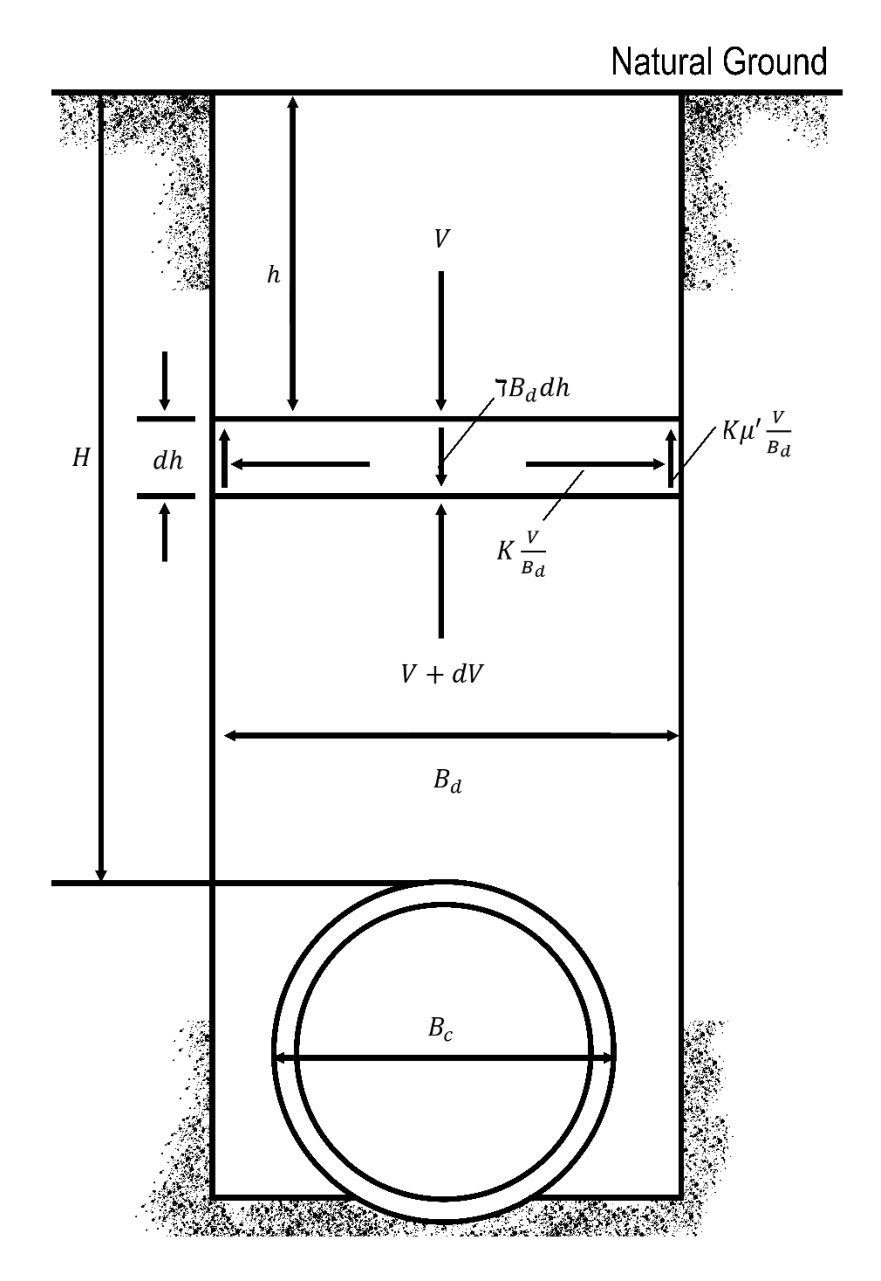


Figure 8. Basis for Marston Theory (Recreated Figure based on [13])

Table 5 shows typical values of  $K\mu'$  for some soil types. The active soil pressure coefficient can also be calculated using Rankine's theory [32]. For a cohesionless soil, this coefficient can be calculated from **Equation 36**:

$$K = \frac{1 - \sin \varphi'}{1 + \sin \varphi'}$$
 Equation 36

The  $\varphi'$  in **Equation 36** is the effective angle of internal friction of the soil. The soil friction angle is a fundamental property in soil mechanics that describes the shear strength of soil due to internal friction between soil particles. The soil friction angle is the angle at which soil particles resist sliding over each other due to friction.

Figure 9 and Figure 10 show comparisons between the Marston and Prism load theories, respectively, for a flexible and a rigid pipe. In these figures, the horizontal axis represents the ratio of pipe depth to outer diameter (OD), while the vertical axis represents the ratio of Marston soil pressure to that of the Prism load. Each figure contains 4 different trench widths ranging from OD to six times the OD.

Table 5. Typical Values for Soil  $K\mu'$ 

Soil Classification	Value
Partially compacted damp topsoil	0.5
Saturated topsoil	0.4
Partially compacted damp clay	0.4
Saturated clay	0.3
Dry sand	0.5
Wet sand	0.5

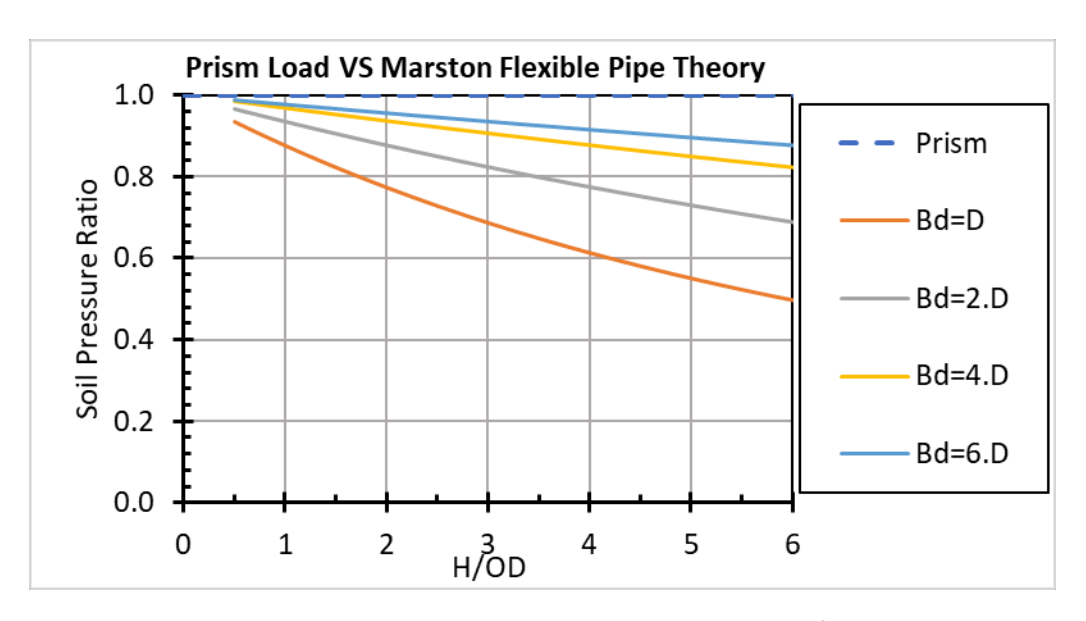


Figure 9. Marston Versus Prism Load Soil Pressure Comparison for a Flexible Pipe

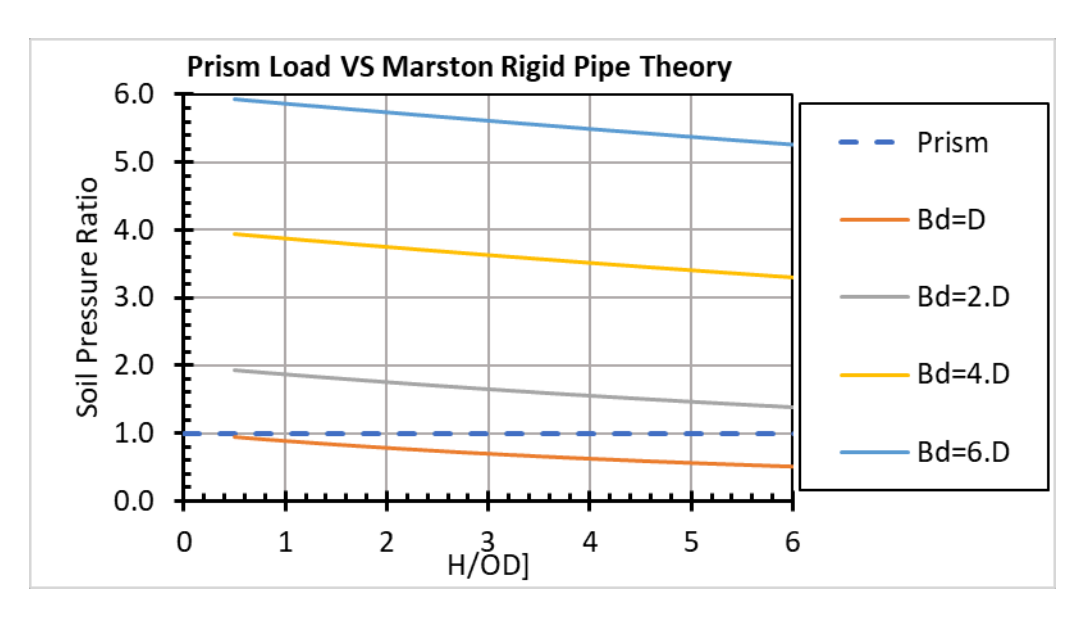


Figure 10. Marston Versus Prism Load Soil Pressure Comparison for a Rigid Pipe

The Marston model assumes that the ditch has vertical sides. The Marston model has been extended to inclined ditches by Li and Dube in 2013 [33].

Based on the above discussion, it is recommended to use the Prism Load method with or without the lateral pressure coefficient for pipelines with shallow cover depths (less than or equal to 1 m). For greater cover depths, the Marston model can be used to achieve higher accuracy. Steel pipelines can generally be treated as flexible pipes.

#### 3.3 E'Value

As shown in Table 1, the recommended E' values are functions of soil classification, cover depth, and soil compaction. The tabulated values exhibit discontinuity as these parameters change. Since mathematically continuous results are more desirable for the decision-making process, interpolation can be used to express variation of E' with cover depth, compaction degree, and percentage of fines in the soil. The following equations are based on the tabulated values in Table 1:

$$E' = E_1(H^{0.2})0.0012 \cdot e^{7.85 \cdot c}$$
 [psi] Equation 37

 $E_1 = 500 + (1 - f)200$  [psi] Equation 38

where

c is the backfill compaction degree,  $0.85 \le c \le 1.0$ 

f is the weight fraction of fines in the backfill soil,  $0 \le f \le 1$ 

*H* is pipe cover depth in ft.

Note that in the above equation, the E' is in psi. The above equation has a maximum error of 15% compared to the tabulated values, which is insignificant considering the intrinsic subjectiveness of E'

determination. The main advantage of using interpolation is that it reduces user dependency of the surface loading calculations by relating E' to soil parameters that can be determined experimentally. The operating companies may use the above correlation or develop similar correlations or continue to use the tabulated values.

## 3.4 Longitudinal Stresses

Global bending stress can be calculated using the beam-on-elastic-foundation theory (e.g., see [6]) without invoking the equivalent point load method. The bending moment in a straight infinite beam-on-elastic-foundation, shown in Figure 11, is calculated as follows:

$$M(x) = D \int_{x_1}^{x_2} \frac{w(\xi)}{3\beta} \left( \cos(\beta|x - \xi|) + \sin(\beta|x - \xi|) \right) e^{-\beta|x - \xi|} \cdot d\xi$$
 Equation 39

where

D is the pipe OD e is the Euler's number (2.718281...)

x is the axial location of the measurement point

 $\xi$  is an integration variable representing axial distance along the beam

w is the distributed load over the pipeline

 $\beta$  is a beam on elastic foundation parameter defined as  $\beta=\sqrt[4]{rac{k}{4EI}}$ 

k is soil spring constant per unit length of the pipe

I is the second moment of area for the pipe section calculated as  $I = \frac{\pi}{64}(D^4 - (D-2t)^4)$ .

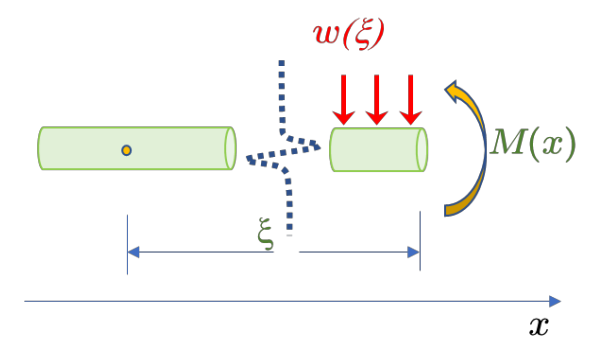


Figure 11. Beam on Elastic Foundation

The soil spring stiffness, k, can be calculated from a suitable method by the analyst and entered in the spreadsheet. Vessic's equation [34] is one of the methods:

$$k = 0.65 \left(\frac{E_{soil} \cdot D}{EI}\right)^{0.083} \frac{E_{soil}}{1 - v_{soil}^2}$$
 Equation 40

In **Equation 40**  $E_{soil}$  and  $v_{soil}$  are the elastic modulus and Poisson's ratio of soil, respectively, I is the second moment of area of the pipe section and D is the pipe outer diameter. Note that the soil elastic modulus,  $E_{soil}$ , is generally different from the modulus of soil reaction, E'. Table 4 contains typical values for the soil Poisson's ratio. Table 6 to Table 9 contain typical elastic moduli for various soil classifications. These values are provided to serve as a guide only. It is recommended to collect representative soil data for analysis.

**Equation 39** does not have a universal solution for a general loading distribution w(x). Thus, numerical integration is used as the primary method to calculate the bending moment diagram in the pipeline. The length of the pipe is divided into shorter segments, typically one or two times the outer diameter (OD) of the pipe. The distribution of soil load across each pipe segment is determined using Boussinesq's equation. Afterwards, the expression under the integral is assessed for each segment. Standard integration techniques, like the midpoint Rule or Trapezoidal Rule, are applied to compute the bending moment along the pipe. References [21, 22, 25] provide details on how to implement **Equation 40**].

Another method to determine soil spring constant is the American Lifelines Alliance soil spring model [35]. The soil spring constant is primarily controlled by the soil layer directly under the pipeline. This method requires soil shear strength properties. Table 10 lists typical values for several different soil classifications.

Table 6. Typical Elastic Moduli for Granular Soil in psi [36]

USCS designation	Loose Soil	Medium Soil	Dense Soil
Well graded gravel	7975	17400	29000
Poorly graded gravel	4785	10440	17400
Silty gravel	1378	2320	4350
Clayey gravel	1378	2320	4350
Well graded sand	4350	11600	23200
Poorly graded sand	2900	5800	9425
Silty sand	1015	1740	2900
Clayey sand	1015	1740	2900

Table 7. Typical Elastic Moduli for Granular Soil in MPa [36]

USCS designation	Loose Soil	Medium Soil	Dense Soil
Well graded gravel	55	120	200
Poorly graded gravel	33	72	120
Silty gravel	9.5	16	30
Clayey gravel	9.5	16	30
Well graded sand	30	80	160
Poorly graded sand	20	40	65
Silty sand	7	12	20
Clayey sand	7	12	20

Table 8. Typical Elastic Moduli for Cohesive Soil in psi [36]

USCS designation	Very Soft to Soft Soil	Medium Soil	Stiff to Very Stiff Soil	Hard Soil
Silt	761	1813	3915	8700
Lean clay	435	1160	2900	6525
Organic silt	73	392	537	682
Plastic silt	580	1015	2900	4350
Plastic clay	290	798	1885	3625
Organic clay	73	290	435	580

Table 9. Typical Elastic Moduli for Cohesive Soil in MPa [36]

USCS designation	Very Soft to Soft Soil	Medium Soil	Stiff to Very Stiff Soil	Hard Soil
Silt	5.3	12.5	27.0	60.0
Lean clay	3.0	8.0	20.0	45.0
Organic silt	0.5	2.7	3.7	4.7
Plastic silt	4.0	7.0	20.0	30.0
Plastic clay	2.0	5.5	13.0	25.0
Organic clay	0.5	2.0	3.0	4.0

Table 10. Typical Values for Soil Friction Angle and Cohesion

Soil Type	Friction Angle (degrees)	Cohesion (psi)	Cohesion (kPa)
well-graded gravel	38	0	0
poorly graded gravel	36	0	0
silty gravel	36	0	0
clayey gravel	32	1.45	10
well-graded sand	34	0	0
poorly graded sand	30	0	0
silty sand	30	0	0
clayey sand	30	1.45	10
silt with low plasticity	28	0	0
lean clay	28	2.175	15
organic silt, organic clay with low plasticity	22	1.45	10
plastic silt	26	1.45	10
fat clay	20	2.175	15
organic clay, organic silt	18	2.175	15

# 3.5 Bedding Angle

The bedding angle should be determined by the analyst based on engineering judgment and an understanding of the pipeline and soil conditions. Based on the 2005, 2006, and 2009 CEPA documents [2, 3, 18] and other references such as [7, 24, 35] the following values are recommended when no additional information about the bedding conditions of a pipeline is available:

- 0° for pipe laid in a rock trench
- 0° for pipe laid in an open trench and backfilled with a loose fat clay (high plasticity clay)
- 30° for a recent open trench construction with a loose, low plasticity cohesive backfill
- 30° to 60° for compacted clay
- 60° for compacted clay when the soil has been given enough time to consolidate (usually longer than 5 years)
- 60° to 90° for pipe installed in open trench with non-cohesive granular backfill
- 90° for designed backfill to ensure good bedding at the time of construction
- 90° for bored pipe and deeply buried pipe
- 180° for flowable fill backfill

Operating companies should develop their own specifications to guide their engineers select an appropriate bedding angle. The decision on proper selection of bedding angle should account for

construction practices and methods regarding pipe fitting, bedding preparation, and backfill placement and compaction that an operator has historically implemented.

## 3.6 Impact Factor

API RP 1102, the 2009 CEPA report [18], and the ENV-6 reports [7], [24] minimum impact factors of 1.5 and 1.75 are recommended, respectively for road vehicles and railroad. According to API 1102, the impact factor can be reduced by 0.1 per meter of depth below 1.5 m (0.03 per foot below 5 ft cover depth) until the impact factor equals 1.

- For low speed (< 15 kph) agricultural vehicles with low tire pressure (<206 kPa) a lower impact factor of 1.25 can be used.
- Based on the PRCI ENV-6-1 project, the following recommendations are made for construction equipment:
- For construction vehicles with high tire pressure that tend to generate impact (loader with load) a higher impact factor of 2 is recommended.
- For track vehicles, it is recommended to use an impact factor equal to or greater than 2 or, alternatively, distribute the load over a portion of the track length (50% or less, depending on road roughness) to account for dynamic effects and non-uniform load distribution.

# 3.7 General Load Footprint and Crossing Angle

A load matrix was one of the options to enter vehicular footprint into the legacy CEPA Calculator. Figure 12 shows an example of a load matrix.

F,	Χ,	Υ,
kN	m	m
17.793	0.000	-0.914
17.793	0.000	0.914
71.172	4.267	-0.914
71.172	4.267	0.914

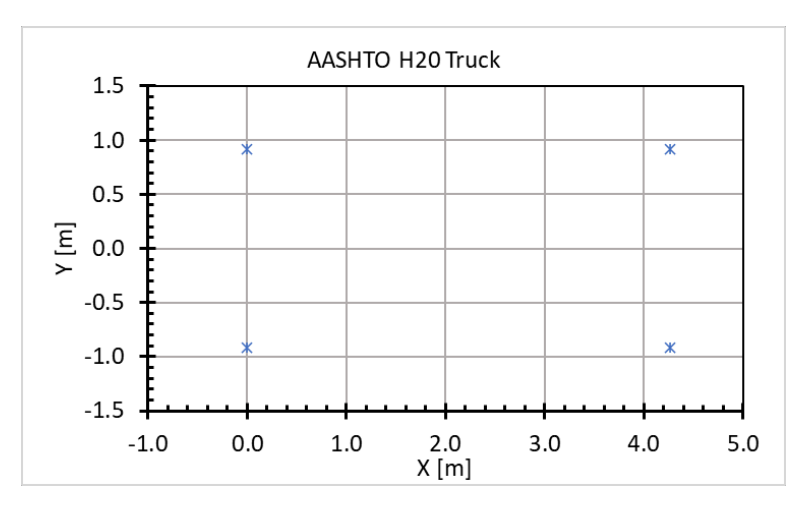


Figure 12. Vehicle Load Matrix for AASHTO H₂O Truck

The load matrix feature offers extensive flexibility for entering vehicle information. Users can specify various vehicle categories, including various legal axle configurations, multi-axle vehicles (e.g., trailers, trains), several side-by-side vehicles, agricultural machinery, roller compactors, or even objects with arbitrary footprints. In the legacy CEPA calculator the user was required to enter the location of the measurement point by specifying its (x, y) coordinates. The measurement point should generally be the point at which the soil pressure from the live load is the maximum value. However, the legacy CEPA Calculator did not provide a function to determine this critical point.

Figure 13 shows soil pressure under a vehicle with two axles and four wheels carrying equal loads at cover depths of 2 m and 3 m. As seen in the figure the increase in the cover depth has shifted the location of the critical point from under the wheels to the center of the vehicle. This example shows it is not always possible to intuitively determine the critical location, because it is not always under the heaviest load.

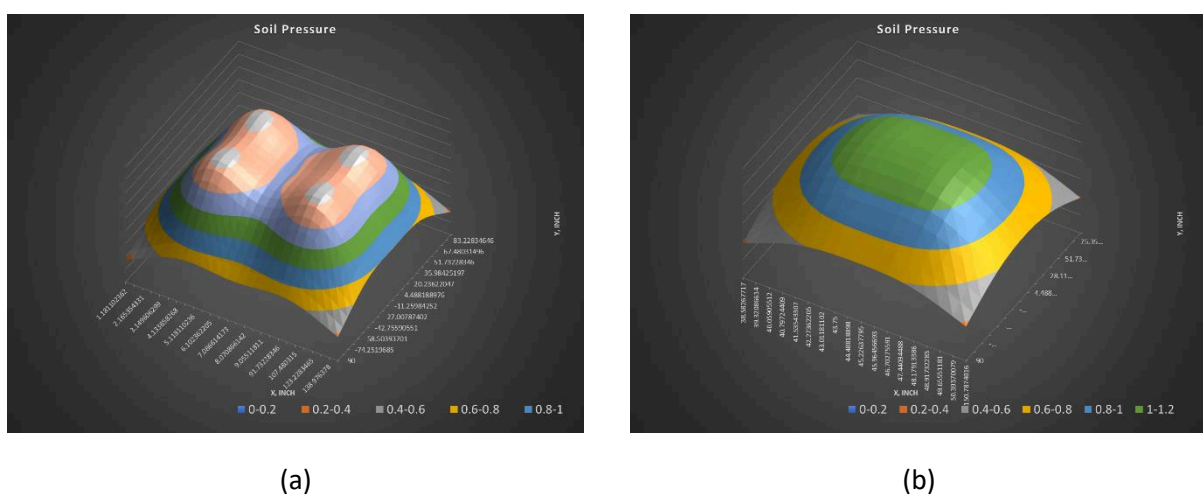


Figure 13. Vehicle Load Matrix for an Equipment with Two Axles and Equal Wheel Loads:
(a) At a Cover Depth of 2 m and (b) at a Cover Depth of 3 m

To effectively analyze a general surface loading crossing, it is advisable to conduct soil pressure calculations over a dense grid that encompasses the entire footprint to determine the critical point. This process may require significant computational resources, which underscores the need for automation.

Another advantage of using load grid combined with automatic calculations is that it allows a user to define crossings with an angle other than perpendicular. Figure 14 shows a crossing with an arbitrary angle. For an angled crossing, the load matrix can be rotated using a planar transformation matrix to align it with the orientation of the vehicle. Figure 15 shows another useful configuration with a vehicle running parallel to the pipeline at some offset distance. This configuration arises when a pipeline is installed near the shoulders of a road or railroad. For surface loading analysis of a pipeline with a parallel configuration, the critical point search window should be limited to a line parallel to the pipeline with the respective offset distance.

<sup>&</sup>lt;sup>9</sup> Refer to Figure 17 of Paper No. IPC2024-133500 for illustration of different crossing angles from zero to 180 degrees.

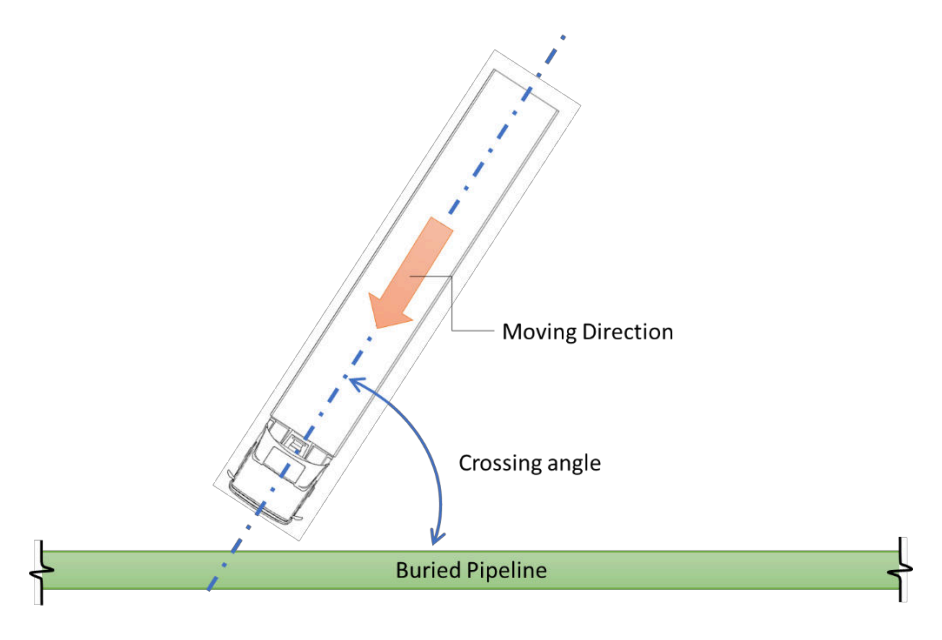


Figure 14. Crossing with a Fixed Angle

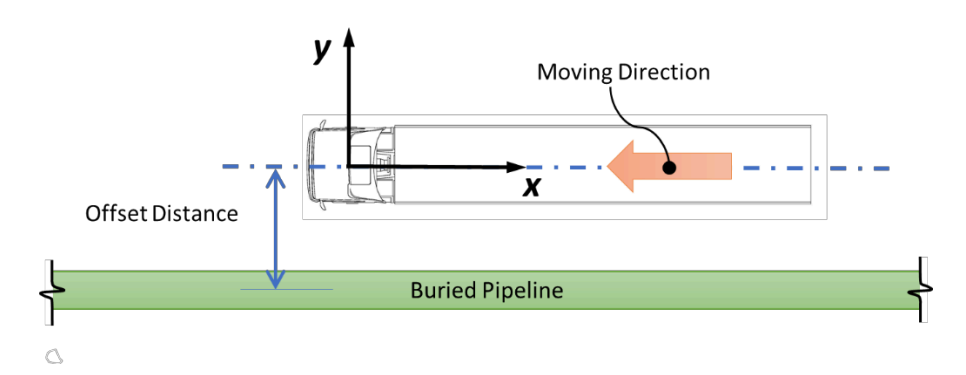


Figure 15. Parallel Configuration

TC Energy has pioneered using coordinate transformation to calculate vehicular load matrices for angled crossings. Details of the implementation of an angled load matrix can be found in a published IPC paper [21].

# 3.8 Vibratory Compactor

To model a vibratory compactor with vibration 'on', it is recommended to add the centrifugal force to the static drum weight. When the centrifugal force is included, the impact factor can be set to 1 for the drum [7]. However, an impact factor of 1.5 should still be applied to any axle load. This impact factor can be reduced when the cover depth is greater than 1.5 m (5 ft) in accordance with the API RP 1102 method.

This method replaces vibratory loads with an equivalent live load. When detailed fatigue assessment is warranted (usually for the case when the live stresses exceed design fatigue endurance limits), a vibration assessment should be performed on the pipeline. Vibration assessment is not in the scope of this document.

#### 3.9 Timber Mat and Slab

The PRCI ENV-6 projects [7], [24], [20] examined the effect of timber mat, road plate, and air-bridge (collectively known as the means of temporary crossing) on the surface loading stress distribution. Both the ENV-6-1 and ENV-6-2 projects revealed that timber-mat is not very effective when placed parallel to the pipeline. Timber-mats could be effective in reducing surface loading stresses when placed perpendicular to the pipeline and when the mats are sufficiently long. For example, the short timber-mats (4-ft-log in the direction perpendicular to the pipeline) installed over the 12-inch pipe specimen in the ENV-6-2 project did not reduce the surface loading stresses, and in some instances increased the stresses. Similarly, timber-mats placed parallel to the pipe specimens in the ENV-6-1 project increased the surface loading-induced stresses under track vehicles.

The outcomes of the ENV-6-2 project also showed that road plates were not very efficient in reducing surface loading stresses. Road plates can still be used to prevent soil erosion and rut development at pipeline crossings.

A detailed model to calculate load distribution under unidirectional (e.g. timber mat) or bidirectional (e.g. slab) layer placed on the surface was discussed in IPC 2020 [37]. The model uses beam-on-elastic-foundation theory (Figure 16) to derive and solve the equation for a stiff layer over a softer soil. A detailed description of the model can be found in Reference [37]. The final solution for the model is as outlined in the following lines:

$$u = \frac{h * \psi_v}{4\beta^3} + \psi_u u_0 + \frac{\psi_\theta}{2\beta} \theta_0$$
 Equation 41

$$u_0 = \frac{C_\theta a_m - C_u a_v}{2\beta a_m^2 - \beta a_v a_\theta}$$
 Equation 42

$$\theta_0 = \frac{2C_u a_m - C_\theta a_\theta}{2a_m^2 - a_v a_\theta}$$
 Equation 43

$$w(x) = -k \cdot u(x)$$
 Equation 44

where

E is modulus of elasticity of slab or plate

 $E_s$  is elastic modulus of soil in contact with slab or plate

I second moment of area of beam (i.e. timbers of slab)

k soil stiffness factor

u is deflection of the beam (i.e. timbers or slab)

 $u_0$  is deflection of the beam at x=0

w contact load distribution between a temporary crossing

 $\beta$  is soil stiffness factor in beam-on-elastic-foundation theory:  $\beta = \sqrt[4]{\frac{k}{4EI}}$ 

 $\theta_0$  is beam slope of deformation at x=0, and

The  $\psi$  functions are defined as:

$$\psi_v = \cosh(\beta x) \sin(\beta x) - \sinh(\beta x) \cos(\beta x)$$

$$\psi_u = \cos(\beta x) \cosh(\beta x)$$

$$\psi_\theta = \cosh(\beta x) \sin(\beta x) + \sinh(\beta x) \cos(\beta x)$$

$$\psi_m = \sinh(\beta x) \sin(\beta x)$$

While the remaining parameters are defined as

$$C_{\theta} = \int_{0}^{L} h(L - \xi) \cdot \psi_{\theta}(\xi) \cdot d\xi$$

$$C_{u} = \int_{0}^{L} h(L - \xi) \cdot \psi_{u}(\xi) \cdot d\xi$$

$$a_{v} = 2\beta^{2} \psi_{v}|_{x=L}$$

$$a_{\theta} = 2\beta^{2} \psi_{\theta}|_{x=L}$$

$$a_{m} = 2\beta^{2} \psi_{m}|_{x=L}$$

where

$$h(x) = \frac{-q(x)}{EI}$$

h(x) represents the vehicular load on the timber mat or slab. The above equations represent a general solution for a load, q(x), with an arbitrary distribution. A vehicular footprint can usually be approximated as a set of concentrated loads. Using this approximation and the superposition principle, the solution can be greatly reduced.

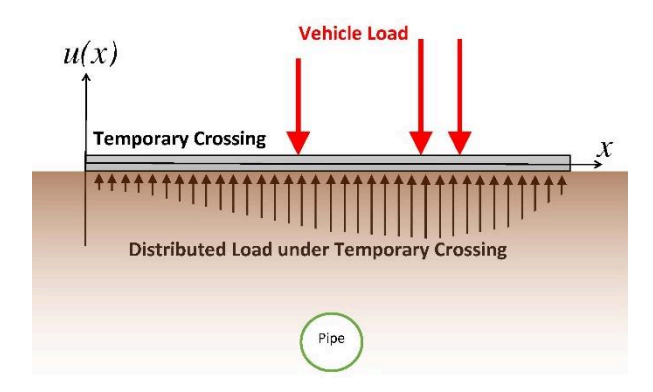


Figure 16. Beam-on-Elastic-Foundation Model for the Analysis of Timber Mat

For a point load, F, acting at distance a from the left end of the beam using the properties of the Dirac delta function:

$$C_{\theta} = \frac{-F}{EI} \cdot \psi_{\theta}(L - a)$$
 Equation 45

$$C_u = \frac{-F}{EI} \cdot \psi_u(L-a)$$
 Equation 46

Similarly, the convolution integral in Equation 41 can be simplified as:

$$h * \psi = \begin{vmatrix} 0 & \text{if } x < a \\ \frac{-F}{EI} & \psi(x - a) & \text{if } x \ge a \end{vmatrix}$$
 Equation 47

This model requires elastic modulus of the means of crossing i.e. timber mat, road plate, or concrete slab. Elastic modulus for a road plate made of structural steel can be taken to be 2.97E+7 psi (205,000 MPa). The elastic modulus of concrete can be calculated from one of the following equations:

$$E_{concrete} = 57000\sqrt{f_c'}$$
 [psi] Equation 48

$$E_{concrete} = 4700\sqrt{f_c'}$$
 [MPa] Equation 49

where  $f_c'$  is the compressive strength of concrete in psi (Equation 48) or MPa (Equation 49).

Table 11 contains elastic moduli for various wood types.

Table 11. Typical Elastic Moduli along Fibers for Wood [38]

Matarial	E	E
Material	(psi)	(MPa)
Pine wood	1,305,000	9000
Alder, red	1,377,500	9500
Ash, white	1,740,000	12000
Basswood, American	1,464,500	10100
Beech, American	1,725,500	11900
Birch, yellow	2,015,500	13900
Maple, sugar	1,827,000	12600
Cherry, black	1,493,500	10300
Cottonwood, eastern	1,363,000	9400
Elm, rock	1,537,000	10600
True hickory, shagbark	2,160,500	14900
Oak, white, red, northern	1,783,500	12300

Walnut, black	1,682,000	11600
Tupelo, black	1,203,500	8300

For details on how to implement this model into a surface loading analysis tool, refer to the published paper [37].

Given the complexity of the RSI model, operating companies may choose to use some other simplified models. For example, a modified CEPA model developed by an ECC operating company accounts for protection measures such as timber mats. Details of the modified CEPA model can be found in Reference [22].

#### 3.10 Effect of Road Pavement

When a pipeline crosses a paved roadway, the load-spreading effect of pavements can be accounted for using the methods discussed in Section 2.10 or Section 3.9 for slabs. The load-spreading effect of a road pavement is similar to a slab, with an elastic modulus that represents the stiffness of asphalt or concrete pavement. When the elastic modulus of asphalt pavement is assessed, the effect of temperature should be accounted for, as warmer temperatures can significantly reduce the elastic modulus of asphalt.

## 3.11 Assessing Pipe Anomalies for Surface Loading

Anomalies such as metal loss, cracks, dents, other deformation features, and imperfections in girth and seam welds can negatively affect the pipeline's allowable limits. The general method for addressing pipe anomalies is through a Fitness-for-Service (FFS) assessment.

The 2009 CEPA report [18] contained a flow diagram titled "Pipeline Surface Loading Acceptability Process Flow Diagram" that illustrated the recommended process for determining the acceptability of surface loading (see Figure 17). This diagram included a "Static Stress Demand - Capacity Check" which incorporates a "Condition Factor" (CF). The Condition Factor was used to account for the pipeline's condition, with different values assigned based on the presence of anomalies.

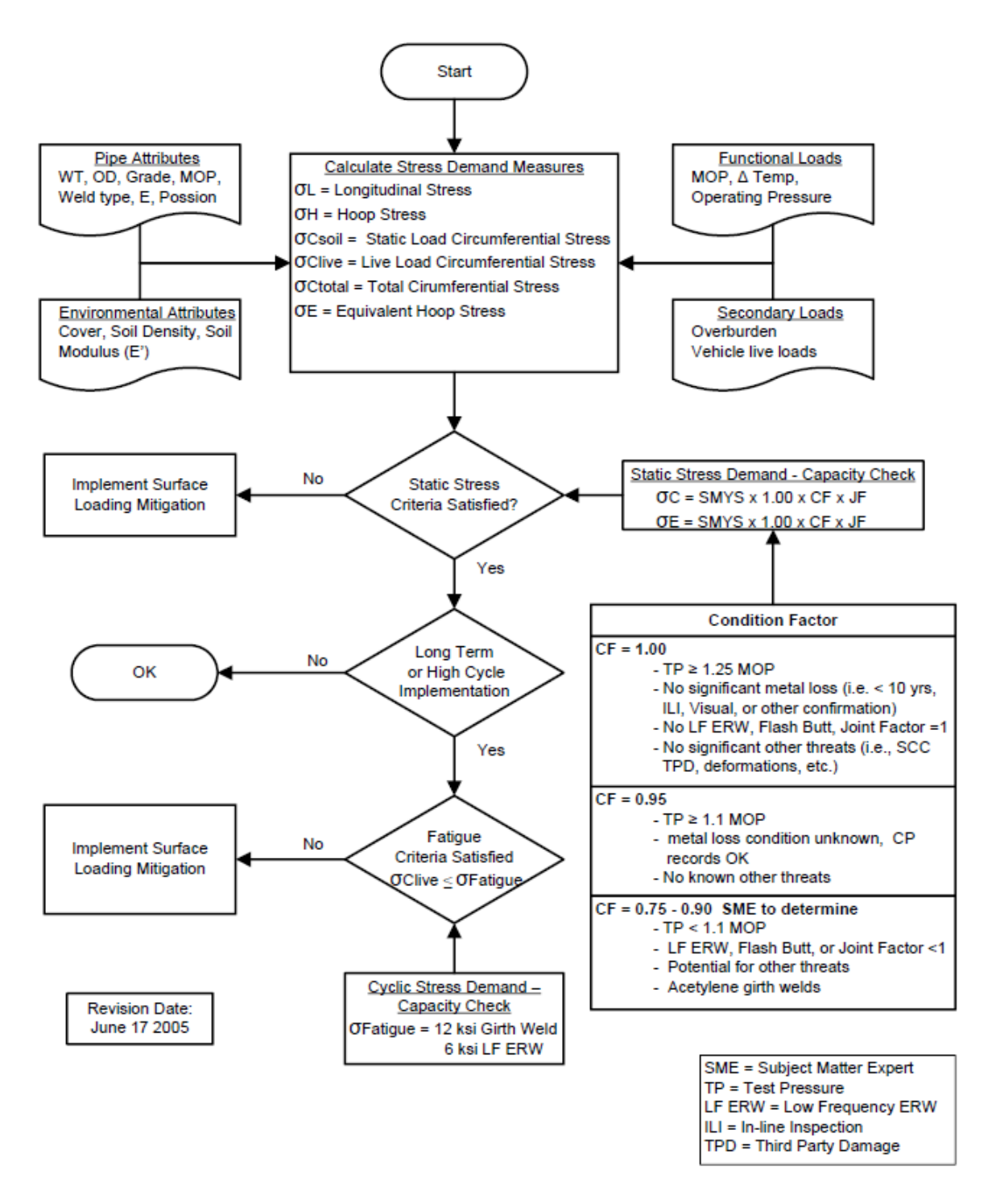


Figure 17. Pipeline Surface Loading Acceptability Process Flow Diagram [18]

CF = 1.00: This factor applies if there is no significant metal loss (e.g., less than 10 years of data from an in-line inspection), no low-frequency electric-resistance weld (LF ERW) or flash butt weld, a joint factor of 1, and no other significant threats like stress corrosion cracking (SCC), third-party damage (TPD), or deformations.

CF = 0.95: This factor is used when the metal loss condition is unknown, but cathodic protection (CP) records are in good order, and there are no other known threats.

CF = 0.75 - 0.90: The selection of a value within this range is determined by an SME. This range applies to situations where the test pressure is less than 1.1 times the maximum operating pressure (MOP), the pipe has LF ERW, flash butt, or a joint factor less than 1, there is a potential for other threats, or if there are acetylene girth welds.

While the above method can be used as a screening tool when no ILI data are available or when surface loading-induced stresses are low (<10% SMYS), more comprehensive and dedicated FFS assessments are recommended for the surface loading analysis when low cover depths or heavy vehicles are involved. The FFS process allows the designer to evaluate these imperfections and, if necessary, provide additional strength or protection against potential damage modes. This is particularly important because, while CSA Z662:23 outlines design requirements for operational and thermal loads, it explicitly states that additional loadings like excessive overburden and cyclical traffic loads are not specifically addressed within the standard<sup>10</sup>. Therefore, the designer must determine if supplemental design criteria are needed for such loads.

The reports also highlight that certain pipe seam types, such as low-frequency ERW and electric flash weld, may be susceptible to seam failures. Operating companies should consider this susceptibility if heavy equipment crosses the pipeline at high frequencies.

When the axial locations of the anomalies are known with a high level of confidence, the potentially negative effect of each anomaly can be limited to its location. Using a similar approach is generally not recommended for the circumferential location of an anomaly because the orientation of pipe ovalization changes as a crossing vehicle approaches the pipeline. Furthermore, a review of the experimental data from ENV-6-1 and ENV-6-2 [7, 24, 20] projects show that the circumferential location of the maximum tensile and compressive stresses was not always consistent with vertical ovalization of the pipes.

For the FFS assessment of pipelines subject to such condition, API 579 [38] is a recommended practice that includes FFS procedures for cylindrical pressure vessels. In many cases, a Level 1 or Level 2 FFS is adequate. However, sometimes it may become necessary to conduct a Level 3 assessment, which includes a detailed finite element analysis. Here we have outlined a proposed FFS for anomalies.

FFS of pipeline anomalies under surface loading should be performed by an SME.

#### 3.11.1 Data Requirements for FFS Assessments

This would be a valuable addition. The text mentions "ILI data" and "CP records" but does not elaborate on the full scope of data needed for a robust FFS. This new section could list key data points:

- Inspection data including ILI data and NDE data
- Hydrostatic test pressure history

51

<sup>&</sup>lt;sup>10</sup> Refer to Clause 4.3.1.1 of CSA Z662:23.

- Operating pressure and temperature data
- Pipe material specifications (SMYS, SMTS, toughness)
- Weld procedures and inspection reports
- Historical repair records
- Soil conditions and cover depth.

#### 3.11.2 Metal Loss in Base Metal

The effect of a metal loss or a cluster can be accounted for by calculating plastic collapse capacity of the pipeline in the circumferential and longitudinal directions, using the modified ASME B31.G method [39] and the modified Miller's solution in Annex A of API 1104 [40], respectively.

The plastic collapse stress in the circumferential direction is calculated as:

$$\sigma_{cH} = \sigma_f \frac{1 - 0.85\eta}{1 - \frac{0.85\eta}{M}}$$
 Equation 50 
$$M = \sqrt{1 + 0.6275z - 0.003375z^2} \quad \text{if} \quad z \le 50$$
 Equation 51 
$$M = 0.032z + 3.3 \quad \text{if} \quad z > 50$$
 Equation 52 
$$z = \frac{L^2}{D \cdot t} \quad \text{if} \quad z \le 50$$
 Equation 53

Where

*D* is pipe outer diameter;

L is metal loss length (in the axial direction of the pipe);

t is pipe wall thickness;

 $\eta$  is anomaly depth to pipe wall thickness ratio ( $\eta = d/t$ ); and

 $\sigma_f$  is the pipe flow stress, which is calculated as the pipe SMYS plus 10,000 psi for the circumferential collapse load calculations.

The plastic collapse stress in the longitudinal direction is calculated as:

$$\sigma_{cL} = \left(\frac{\pi}{4} + 385(0.05 - \eta \cdot \beta)^{2.5}\right) \left(\cos\left(\frac{\eta \cdot \beta \cdot \pi}{2}\right) - \frac{\eta \cdot \sin(\beta \cdot \pi)}{2}\right) \sigma_{y}$$
 Equation 54 if  $\eta \cdot \beta < 0.05$ 

$$\sigma_{cL} = \frac{\pi}{4} \left( \cos \left( \frac{\eta \cdot \beta \cdot \pi}{2} \right) - \frac{\eta \cdot \sin \left( \beta \cdot \pi \right)}{2} \right) \sigma_{y} \quad \text{if} \quad \eta \cdot \beta \geq 0.05$$
 Equation 55

The stress ratio in the longitudinal direction is given as:

$$L_r = \frac{\sigma_L}{\sigma_{cL}}$$
 Equation 56

The stress ratio is deemed acceptable when it is equal to or less than the cut-off limit:

$$L_r^{cutoff} = \frac{\sigma_f}{\sigma_y}$$
 Equation 57

In the above equations  $\sigma_y$  is the pipe SMYS, anomaly depth ratio,  $\eta$ , is as previously defined, and  $\beta$  is the anomaly width (in the circumferential direction) to pipe circumference ratio:

$$\beta = \frac{w}{\pi \cdot D}$$
 Equation 58

The flow stress,  $\sigma_f$ , can be calculated as the average value of SMYS and the specified minimum tensile strength (SMTS) of the pipe.

#### 3.11.3 Metal Loss with Weld Interaction

The presence of metal loss on a girth weld or seam weld can affect fatigue life, fracture resistance, and plastic collapse strength of the girth weld.

This approach in this section does not apply to selective seam weld corrosion anomalies. Operating companies should determine the proper mitigation strategy in such cases.

A conservative method to assess a weld with metal loss under surface loading is discussed in Annex K of CSA Z662:23 or Annex A of API 1104. Similar models based on failure assessment diagram (FAD) for static load and a crack growth model for live load cycles can also be used. If the metal loss fails the assessment, then a fracture mechanics-based numerical analysis (e.g., API 579) can be performed.

The FFS assessment should account for all the known stresses, including the surface loading-induced stresses. When the crossing is a permanent crossing, crack growth due to stress cycles from live surface load or other sources may need to be addressed.

#### 3.11.4 Crack-Like Features

Crack-like features can be assessed following a fracture mechanics-based FFS assessment method, such as presented in API 579 or Annex J and Annex K of CSA Z662:23.

The FFS assessment should include all known stresses, including surface loading-induced stresses in the longitudinal and/or circumferential directions. When the crossing is a permanent crossing, crack growth due to live load cycles, as well as other cyclic loads, should be addressed in the assessment.

## 3.11.5 Dent, Mechanical Damage, and Deformation Features

Dents, deformation, and mechanical damage can act as stress concentrators, significantly reducing the pipeline's fatigue life and making it more susceptible to failure under cyclical loads from traffic. The reduced cross-section and altered geometry can also compromise the pipeline's compressive and bending strength, which are critical for resisting surface loading. Buckling resistance of a pipeline is particularly sensitive to the presence of dents and other forms of deformation due to the eccentricity they introduce.

Currently, there is no industry-wide guidance on how to assess the bending resistance or compressive resistance of a pipe with a dent or deformation. Therefore, the only reliable assessment method is dedicated numerical analysis.

# 4 References

- [1] API 1102-2007, "Steel Pipelines Crossing Railroads and Highways," American Petroleum Institute, 2007 with Errata until 2010.
- [2] D. J. Warman and D. J. Hart, "Development of a pipeline surface loading screening process & assessment of surface load dispersing methods," Kiefner and Associates, Inc. for Canadian Energy Pipeline Association (CEPA), June 2005.
- [3] D. J. Warman, J. Chorney, M. Reed and J. Hart, "Development of a pipeline surface loading screening process (IPC2006-10464)," in *6th International Pipeline Conference*, Calgary, Alberta, Canada, September 25-29, 2006.
- [4] M. Van Auker and B. Francini, "Canadian Energy Pipeline Association (CEPA) surface loading calculator user manual," Kiefner and Associates, Inc., January 28, 2014, Final Report No. 14-017.
- [5] R. K. Watkins and M. G. Spangler, "Some charachteristics of the modulus of passive resistance of soil: A study in similitude," in *Proceedings of the 37th Annual Meeting, Highway Research Board (HRB)*, Washington DC, 1958.
- [6] A. P. Boresi, R. J. Schmidt and S. M. Omar, Advanced mechanics of material, ISBN 0-471-55157-0, John Wiley & Sons, Inc., Fifth Edition 1993.
- [7] PRCI ENV-6-1, "Field validation of surface loading stress calculations for buried pipelines Milestone 2," Kiefner and Associates for Pipeline Research Council International, Inc (PRCI), Authored by Zand, B., Branam, N. and Webster, W., Report RP-218-104509, April 2018.
- [8] R. Walker, M23 PVC pipe:design and installation, American Water Work Association (AWWA), Third Edition, 2020.
- [9] Plastic Pipe Institute, "Handbook of Polyethylene Pipe," PPI, Second Edition, 2008.
- [10] AWWA M9, Concrete pressure pipe, American Water Works Association, 1995 Second Edition.
- [11] T. Karl, Theoretical soil mechanics, John Wiley and Sons, 1948.
- [12] H.-J. Tien, "A literature study of the arching effect," Massachuset Institute of Technology (MIT), 1996.
- [13] A. P. Moser, Buried pipe design, Mc GrawHill, Second Edition 2001.
- [14] J. C. Potter, "Effects of vehicles on buried, high-pressure pipe," *Journal of Transportation Engineering*, vol. 111, pp. 224-236, 1985.
- [15] J. D. Hartley and J. M. Duncan, "E' and its variation with depth," *Journal of Transportation Engineering*, vol. 113, pp. 538-553, 1987.

- [16] J. K. Jeyapalan and R. Watkins, "Modulus of soil reaction (E') values for pipeline design," *ASCE Journal of transportation engineering*, vol. 130, pp. 43-48, 2004.
- [17] ACPA Design Data 1, "Design Data 1: Highway Live Loads on Concrete Pipe," American Concrete Pipe Association, October 2007.
- [18] D. Warman, J. Hart and R. B. Fracini, "Development of a pipeline surface loading screening process & assessment of surface load dispersing methods," Prepared by Kiefner and Associates for Canadian Energy Pipeline Association (CEPA), Worthington, Ohio, Revised October 16, 2009.
- [19] W. C. Young, R. G. Budynas and A. M. Sadegh, Roark's Formulas for Stress and Strain, Mc Graw Hill, Eighth Edition 2012.
- [20] PRCI ENV-6-2, "Full-Scale surface loading testing of buried pipes," Kiefner and Associates for Pipeline Research Council International, Inc. (PRCI), Report RP-218-174512-R01, June 2021.
- [21] S. Zhang, J. Yan and J. Law, "Advanced surface loading analysis using CEPA model (IPC2024-133500)," in *Proceedings of the 2024 15th International Pipeline Conference*, Calgary, Alberta, Canada, September 23 to 27, 2024.
- [22] S. Zhang, K. Zhang, M. Pino, J. Law and T. Matchim, "Improved surface loading stress analysis method considering protection measures," in *Proceedings of the 2020 13th International Pipeline Conference*, Calgary, Alberta, Canada, September 18 October 2, 2020.
- [23] J. Klementis, S. Zhang, J. Law, M. Pino and J. Yan, "Practical improvements to surface loading assessment-Building accuracy, efficiency and transparency (IPC2018-78633)," in *Proceedings of the 2018 12th International Pipeline Conference*, Calgary, Alberta, Canada, september 24-28, 2018.
- [24] PRCI ENV-6-1, "Field validation of surface loading stress calculations for buried pipelines, Milestone 1," Kiefner and Associates for Pipeline Research Council International, Inc. (PRCI), Report No PR-218-104509-R03, July 2014.
- [25] F. Zhang, N. Branam, B. Zand and M. Van Auker, "A new approach to determine the stresses in buried pipe under surface loading (IPC2016-64050)," in 11th International Pipeline Confrence (IPC) 2016, Calgary, Alberta, Canada, September 26-30, 2016.
- [26] E. A. T. a. H. G. Rodabaugh, "Summary Report on Experimental Evaluation of Simulated Uncased Pipeline Crossings of Railroads and Highways," Battelle Summary Report for Research Council on Pipeline Crossings of Railroads and Highway, ASCE, 1971.
- [27] M. Spangler, "Experimental Study of the Structural Performance of Pipeline Casing Pipes under Railroads and Highways," *Spangler, M.G., "Experimental Study of the Structural Performance of Pipeline CasinJournal of the Pipeline Division, ASCE,* Vols. Spangler, M.G., "Experimental Study of the Structural Performance of Pipeline Casing Pipes u91, No. PL1, Proc. Paper 4419, July, 1965..

- [28] H. I. A. O. T. a. B. Stewart, "Design of Uncased Pipelines at Railroad and Highway Crossing," in *American Petroleum Institute Distribution/Transmission Conference*, Houston, TX, April 7-8, 1992.
- [29] M. Rosenfeld, R. Gailing, B. Zand and J. Anderson, "A Comprehensive Re-evaluation of the Benefits of Pipeline Cover Depth," in *PPIM*, Houston, February 12-16, 2024.
- [30] PROKON, "PROKON Support Portal," [Online].

  Available: https://support.prokon.com/kb/articles/elastic-properties-of-soils. [Accessed 2020].
- [31] Watkins, R.K. and Anderson, L.R, Structural mechanics of buried pipes, CRC Press, 2000.
- [32] W. Rankine, "On the stability of loose earth," Philosophical Transactions of the Royal Society of London, Vol 147, 1856.
- [33] L. Li and J.-S. Dubé, "An extension of Marston's solution for the stresses in backfilled trenches with inclined walls," *Geotechnical and Geological Engineering*, no. 31, p. 1027–1039, August 2013.
- [34] C. M. St John and T. F. Zahrah, "A seismic design of underground structures," *Tunneling Underground Space Technology*, vol. 2, no. 2, pp. 165-197, 1987.
- [35] American Lifelines Alliance, Guidelines for the design of buried steel pipe, American Society of Civil Engineers (ASCE), July 2001 with addenda through February 2005.
- [36] Geotech Data, "Soil Young's modulus," [Online].

  Available: http://www.geotechdata.info/parameter/soil-young-s-modulus. [Accessed 5 2020].
- [37] B. B. Zand, "Vehicle load distribution under timber mats and flexible slabs," in *Proceedings of the 2020 13th International Pipeline Conference*, Calgary, Canada, September 28 to October 2, 2020.
- [38] "Amesweb Advanced Mechanical Engineering Solutions," [Online].

  Available: https://amesweb.info/Materials/Youngs-Modulus-of-Wood.aspx.
- [39] ASME B31G 2023, "Manual for Determining the Remaining Strength of Corroded Pipelines," The American Society of Mechanicsl Engineers, 2023.
- [40] API 1104-2021, "Welding of pipelines and related facilities," American Petroleum Institute, API Standard 1104, Twenty-Second Edition, July 2021.
- [41] ASME B31.8-2022, "Gas Transmission and Distribution Piping Systems," The American Society of Mechanical Engineers (ASME), New York, NY, 2022.
- [42] ASME B31.4-2022, "Pipeline Transportation Systems for Liquids and Slurries," The American Society of Mechanical Engineers (ASME), New York, NY, 2022.
- [43] S. M. Sargand and T. Masada, "Modulus of soil reaction values measured in Ohio thermoplastic pipe deep burial project," *Journal of Pipeline System Engineering and Practice*, vol. 6, 2015.

[44] API 579-1/ASME FFS-1, "Fitness-for-service," American Petroleum Institute and The American Society of Mechanical Engineers, 2021.